fractal and fractional

MDPI

Article

Robust Boundary Intermittent Stabilization of Fractional-Order Memristive Cohen–Grossberg Neural Networks

Muniyappan Madhu [1], Saravanan Shanmugam [2,*], Srinivasan R [1] and Mohamed Rhaima [3,*]

[1] Department of Mathematics, Faculty of Engineering and Technology, SRM Institute of Science and Technology, Ramapuram, Chennai 600089, Tamil Nadu, India
[2] Center for Computational Biology, Easwari Engineering College, Chennai 600089, Tamil Nadu, India
[3] Department of Statistics and Operations Research, College of Sciences, King Saud University, Riyadh 11451, Saudi Arabia
* Correspondence: saravanantvu@gmail.com (S.S.); mrhaima.c@ksu.edu.sa (M.R.)

Abstract

This paper addresses the stabilization problem for a class of fractional-order memristive reaction–diffusion Cohen–Grossberg neural networks with time-varying delays under an intermittent boundary control framework. Two scenarios are considered: systems without parametric uncertainties, for which asymptotic stability is established, and systems with uncertainties, for which robust asymptotic stability is ensured. By constructing appropriate Lyapunov functionals and employing Wirtinger-type inequalities, the fractional Razumikhin approach, and key properties of the Mittag–Leffler function, sufficient stability conditions are derived in terms of linear matrix inequalities with reduced conservatism. Furthermore, the effects of time-varying delays and control activation intervals on the stabilization performance are systematically investigated. The effectiveness and advantages of the proposed control methodology are validated through numerical simulations.

Keywords: fractional-order Cohen–Grossberg neural networks; memristive; reaction–diffusion; uncertain parameters; time-varying delay; intermittent boundary control

1. Introduction

In recent decades, the analysis of the dynamical properties of neural networks (NNs) has become a prominent research topic due to their extensive applications in science and engineering, including intelligent robotics, automatic control systems, associative memory, financial modeling in [1–5], and pattern recognition in [6]. Within this broad class of models, Cohen–Grossberg neural networks (CGNNs) provide a unified, flexible mathematical framework that encompasses several well-known neural architectures, including Hopfield networks [7], cellular neural networks [8], and recurrent neural networks [9]. Since their seminal formulation by Cohen and Grossberg in 1983 [10], CGNNs have been extensively investigated and successfully applied to pattern recognition, parallel computation, and signal and image processing tasks, demonstrating their strong modeling capability and practical relevance.

Another significant development in neural networks is the use of memristive components, which provide memory to the network by encoding activity as resistance states. In particular, fractional-order CGNNs have demonstrated adaptive learning and associative memory capabilities when combined with memristive elements that enable the storage and dynamic modification of weight states [11–13]. Memristors mimic the synaptic plasticity of real biological organisms, so memristive neural networks can also respond adaptively in real time. An extensive review of the dynamic analysis and control of memristive neural

Check for updates

Academic Editors: Ivanka Stamova and António Lopes

Received: 4 February 2026
Revised: 12 March 2026
Accepted: 19 March 2026
Published: 22 March 2026

Copyright: © 2026 by the authors. Licensee MDPI, Basel, Switzerland. This article is an open access article distributed under the terms and conditions of the Creative Commons Attribution (CC BY) license.

networks was conducted by [14]. They examined several control strategies, including multistability, stabilization, synchronization, and the impact of fractional-order dynamics. In the present study, memristors are another important component, inspired by the synaptic plasticity of the human brain, which makes them highly effective in modeling learning behaviors and memory retention [15,16]. In [17], the authors investigated the finite-time stability and synchronization of a fractional-order CGNN based on memristors. By employing Lyapunov functions and a set of control strategies, synchronization and stability are ensured in finite time, addressing both fractional and memristive dynamics. The deformation of finite-time synchronization and stabilization in fractional-order memristor-based CGNNs has thus far predominantly concentrated on ensuring finite-time convergence and robustness with respect to time delays, as seen in the studies by [18,19].

In practical neural network models, reaction–diffusion effects are often incorporated to describe the spatial–temporal evolution of neuron states caused by diffusion mechanisms. Such effects arise from the spatial distribution of electrical signals and interactions between neurons, leading to state variables that depend on both time and space [20–24]. Consequently, reaction–diffusion neural networks provide a more realistic framework to model complex neural dynamics. A substantial number of studies have analyzed neural networks with reaction–diffusion terms, including stabilization and synchronization problems [25–29], as well as extensions involving memristive elements [30–32]. These investigations have contributed to a deeper understanding of neural networks under coupled spatial and temporal dynamics. Moreover, stability analysis of CGNNs delayed in reaction–diffusion settings has been reported in [33]. The problem of synchronization in memristive Cohen–Grossberg reaction–diffusion neural networks subject to time-varying delays was further examined in [34]. Subsequently, fractional-order extensions of these models were considered in [35], where Lipschitz stability criteria were derived for impulsive delayed reaction–diffusion CGNNs.

Two primary control approaches are commonly adopted for reaction–diffusion Cohen–Grossberg neural networks (RDCGNNs), namely distributed control and boundary control (BC). Building on distributed controllers, researchers have developed event-triggered controllers that achieve practical exponential input-to-state stability of stochastic RDCGNNs [36]. However, distributed control can be difficult to implement in many technical applications because actuators must be deployed at every location in the spatial domain. To address this challenge, boundary control has been proposed as an effective alternative for RDCGNNs. Boundary control has been extensively studied because it only requires actuators to be installed at the boundary of the spatial domain. For example, a feedback boundary controller was developed to achieve exponential stability of integer-order RDCGNNs [37]. Despite its effectiveness, BC remains a continuous-time control method, which requires the controller to operate continuously and may result in higher resource and mechanical consumption compared to discontinuous-time controllers. Intermittent control, a special type of discontinuous-time controller [38], can help reduce time costs. Despite these advantages, the stabilization of fractional-order memristive reaction–diffusion Cohen–Grossberg neural networks under boundary control remains largely unexplored. The presence of fractional dynamics introduces additional analytical challenges due to nonlocal memory effects, the involvement of Mittag–Leffler functions, and the need for fractional Razumikhin-type techniques. Moreover, when time-varying delays, memristive switching behaviors, and parametric uncertainties are simultaneously considered, the stability analysis becomes significantly more complicated. Motivated by these challenges, this paper investigates the robust stabilization problem of uncertain fractional-order memristive reaction–diffusion Cohen–Grossberg neural networks under an intermittent boundary control framework. The proposed approach establishes delay-dependent LMI-based conditions that guarantee asymptotic and robust asymptotic stability in the sense of Mittag–Leffler functions. Intermittent boundary control (IBC) has recently

been proposed for integer-order stochastic RDCGNNs with and without time delays [39,40]. To facilitate understanding, Table 1 summarizes recent studies on RDCGNNs with different control strategies and methodologies.

Table 1. Summary of recent studies on RDCGNNs with methodologies and control strategies.

Refs.	Methodology	Control Strategy
[11]	Fractional-order model; Dirichlet boundary condition; algebraic inequality approach; global uniform stability.	State feedback control.
[12]	Fractional-order model; Dirichlet boundary condition; Lyapunov stability theory; LMI approach; Mittag–Leffler stability.	Continuous-time sliding mode control.
[20]	Integer-order model; Dirichlet boundary condition; Lyapunov stability theory; algebraic inequality approach; fixed-time stability.	State feedback control.
[34]	Fractional-order model; memristive term; Dirichlet boundary condition; Lyapunov stability theory; algebraic inequality approach; finite-time stability.	Continuous-time state feedback control.
[36]	Integer-order model; Neumann boundary condition; Lyapunov stability theory; LMI approach; exponential input-to-state stability.	Continuous-time event-triggered control.
[37]	Integer-order model; Neumann boundary condition; Lyapunov stability theory; LMI approach; exponential stability.	Continuous-time boundary feedback control.
[38]	Integer-order model; Dirichlet boundary condition; Lyapunov stability theory; algebraic inequality approach; fixed-time stability.	Discontinuous-time intermittent control.
[39,40]	Integer-order model; Neumann boundary condition; Lyapunov stability theory; LMI approach; exponential stability.	Discontinuous-time intermittent boundary control.
This study	Fractional-order model; memristive term; uncertain parameters; Neumann boundary condition; Mittag–Leffler function; LMI approach; fractional Razumikhin-type theorem; robust asymptotic stability.	Continuous-time boundary control; discontinuous-time intermittent boundary control.

Based on the above discussion, this work investigates the robust stabilization of uncertain fractional-order memristive reaction–diffusion Cohen–Grossberg neural networks (FOMRDCGNNs). By integrating Wirtinger-type inequalities, linear matrix inequality (LMI) techniques and key properties of the Mittag–Leffler function, sufficient conditions ensuring robust stability are derived.

The main contributions of this paper are summarized as follows:

- The stabilization problem of FOMRDCGNNs with time-varying delays is systematically investigated under an intermittent boundary control framework.
- Two practical scenarios are addressed: (i) asymptotic stabilization of networks without parametric uncertainties and (ii) robust asymptotic stabilization of networks in the presence of uncertain parameters.

- By constructing an appropriate Lyapunov functional and employing Wirtinger-type integral inequalities together with the fundamental properties of the Mittag–Leffler function, new delay-dependent stability conditions are derived in the form of linear matrix inequalities (LMIs), which effectively reduce the conservatism of the obtained results.
- The effects of time-varying delays and intermittent control activation intervals on the stabilization performance are explicitly characterized, providing deeper insights for the design and implementation of boundary controllers.
- Finally, numerical simulation examples are presented to demonstrate the effectiveness and feasibility of the proposed control strategy.

2. Problem Description and Preliminaries

Consider the following FOMRDCGNNs with time-varying delays:

$$\begin{aligned} {}_0^C\mathcal{D}_t^{\eta} x(t,\xi) = \mathcal{D}\frac{\partial^2 x(t,\xi)}{\partial \xi^2} - \alpha(x(t,\xi))\big[\beta(x(t,\xi)) - \mathcal{P}(x(t,\xi))f(x(t,\xi)) \\ - \mathcal{Q}(x(t,\xi))g(x(t-\Im(t),\xi))\big]. \end{aligned} \tag{1}$$

subject to the following initial and Neumann boundary conditions:

$$x(\theta,\xi) = \phi(\theta,\xi), \quad \theta \in [-\Im, 0], \tag{2}$$

$$\left.\frac{\partial x(t,\xi)}{\partial \xi}\right|_{\xi=l_1} = 0, \quad \left.\frac{\partial x(t,\xi)}{\partial \xi}\right|_{\xi=l_2} = u(t), \tag{3}$$

where $\xi \in (l_1, l_2)$ and $t > 0$ are the spatial and time variables. The term ${}_0^C\mathcal{D}_t^{\eta} x(t,\xi)$ is known as the fractional Caputo derivative with respect to time t, and the variable $x(t,\xi) = \big(x_1(t,\xi),\ x_2(t,\xi),\ \ldots,\ x_n(t,\xi)\big)^T \in \mathbb{R}^n$ denotes the state of the ith neuron for $i = 1, 2, \ldots, n$. $\phi(\theta,\xi) = \phi_1(\theta,\xi), \phi_2(\theta,\xi), \ldots, \phi_n(\theta,\xi)$.

The diffusion coefficient matrix is denoted by $\mathcal{D} \in \mathbb{R}^{n\times n}$ and is assumed to be positive-definite in accordance with physical principles. The matrices $\mathcal{P}(x(t,\xi)) = [p_{ij}(t,\xi)]_{n\times n}$ and $\mathcal{Q}(x(t,\xi)) = [q_{ij}(t,\xi)]_{n\times n}$ describe the connection weight structure, while $\alpha(\cdot)$ and $\beta(\cdot)$ represent the amplification and behavior functions, respectively.

The neuron activation functions are given by

$$f(x(t,\xi)) = [f_1(x_1(t,\xi)), f_2(x_2(t,\xi)), \ldots, f_n(x_n(t,\xi))]^{\mathrm{T}}$$

and

$$g(x(t-\varsigma(t),\xi)) = [g_1(x_1(t-\Im(t),\xi)), g_2(x_2(t-\Im(t),\xi)), \ldots, g_n(x_n(t-\Im(t),\xi))]^T,$$

which are assumed to be nonlinear and smooth. Furthermore,

$$\alpha(x(t,\xi)) = \mathrm{diag}\{\alpha_1(x_1(t,\xi)), \alpha_2(x_2(t,\xi)), \ldots, \alpha_n(x_n(t,\xi))\},$$

and

$$\beta(x(t,\xi)) = [\beta_1(x_1(t,\xi)), \beta_2(x_2(t,\xi)), \ldots, \beta_n(x_n(t,\xi))]^{\mathrm{T}}$$

denote the corresponding state-dependent functions. The time-varying delay $\Im(t)$ satisfies

$$0 \le \Im(t) \le \Im, \qquad \dot{\Im}(t) \le \varepsilon,$$

where $\bar{\varsigma}$ and ε are known positive constants.

Motivated by the current–voltage characteristics of memristors, state-dependent parameters are introduced to more accurately capture memory effects and pinched hysteresis behavior. Accordingly, the parameters in system (1) are assumed to satisfy the following conditions.

Based on the current–voltage characteristic of a memristor, to more accurately describe its memory function and pinched hysteresis features, the state-dependent parameters in (1) satisfy the following conditions:

$$p_{ij}(x_i(t,\xi)) = \begin{cases} \tilde{p}_{ij}, & \text{sign}_{ij}\,\frac{\partial f_j(x_j(t,\xi))}{\partial t} - \frac{\partial x_i(t,\xi)}{\partial t} < 0 \\ \text{unchanged}, & \text{sign}_{ij}\,\frac{\partial f_j(x_j(t,\xi))}{\partial t} - \frac{\partial x_i(t,\xi)}{\partial t} = 0 \\ \widehat{p}_{ij}, & \text{sign}_{ij}\,\frac{\partial f_j(x_j(t,\xi))}{\partial t} - \frac{\partial x_i(t,\xi)}{\partial t} > 0 \end{cases} \tag{4}$$

$$q_{ij}(x_i(t,\xi)) = \begin{cases} \tilde{q}_{ij}, & \text{sign}_{ij}\,\frac{\partial g_j(x_j(t-\Im(t),\xi))}{\partial t} - \frac{\partial x_i(t,\xi)}{\partial t} < 0 \\ \text{unchanged}, & \text{sign}_{ij}\,\frac{\partial g_j(x_j(t-\Im(t),\xi))}{\partial t} - \frac{\partial x_i(t,\xi)}{\partial t} = 0 \\ \widehat{q}_{ij}, & \text{sign}_{ij}\,\frac{\partial g_j(x_j(t-\Im(t),\xi))}{\partial t} - \frac{\partial x_i(t,\xi)}{\partial t} > 0 \end{cases} \tag{5}$$

where, $\tilde{p}_{ij}, \widehat{p}_{ij}, \tilde{q}_{ij}$, and $\widehat{q}_{ij}$ are constants associated with memristances. Furthermore, the term "unchanged" indicates that the memristance retains its current value. Each parameter can switch between two different constant values: $p_{ij}(x_i(t,\xi))$ can be either $\tilde{p}_{ij}$ or $\widehat{p}_{ij}$, and similarly, $q_{ij}(x_i(t,\xi))$ can be either $\tilde{q}_{ij}$ or $\widehat{q}_{ij}$. Thus, the number of possible combinations of $\mathcal{P}(x(t,\xi))$ and $\mathcal{Q}(x(t,\xi))$ is 2^{2n^2}. These 2^{2n^2} scenarios are ordered as follows:

$$(\mathcal{P}_1, \mathcal{Q}_1), (\mathcal{P}_2, \mathcal{Q}_2), \ldots, \left(\mathcal{P}_{2^{2n^2}}, \mathcal{Q}_{2^{2n^2}}\right).$$

At any fixed time $t \geq 0$, the functions $\mathcal{P}(x(t,\xi))$ and $\mathcal{Q}(x(t,\xi))$ can take on one of 2^{2n^2} possible forms. This means that there exist some $k \in \{1, 2, \ldots, 2^{2n^2}\}$ such that $\mathcal{P}(x(t,\xi)) = \mathcal{P}_k$ and $\mathcal{Q}(x(t,\xi)) = \mathcal{Q}_k$. Based on this analysis, the memristive system described by Equation (1) can be translated into

$${}_0^C\mathcal{D}_t^\eta x(t,\xi) = \mathcal{D}\frac{\partial^2 x(t,\xi)}{\partial \xi^2} - \alpha(x(t,\xi))\left[\beta(x(t,\xi)) - \mathcal{P}_k f(x(t,\xi)) - \mathcal{Q}_k g(x(t-\Im(t),\xi))\right]. \tag{6}$$

Now, for $k = 1, 2, \ldots, 2^{2n^2}$, at any fixed time t, we define the characteristic function of $\mathcal{P}_k$ and $\mathcal{Q}_k$ as follows:

$$\Omega_k(t) = \begin{cases} 1, & \mathcal{P}(x(t,\xi)) = \mathcal{P}_k, \quad \mathcal{Q}(x(t,\xi)) = \mathcal{Q}_k \\ 0, & \text{otherwise} \end{cases} \tag{7}$$

and we can easily conclude that $\sum_{k=1}^{2^{2n^2}} \Omega_k(t) = 1$. Thus, FOMRDCGNNs (1) can be rewritten as

$$\begin{aligned} {}_0^C\mathcal{D}_t^\eta x(t,\xi) = & \sum_{k=1}^{2^{2n^2}} \Omega_k(t)\Big[\mathcal{D}\frac{\partial^2 x(t,\xi)}{\partial \xi^2} - \alpha(x(t,\xi))\left[\beta(x(t,\xi)) - \mathcal{P}_k f(x(t,\xi))\right. \\ & \left. - \mathcal{Q}_k g(x(t-\Im(t),\xi))\right]\Big], \\ = & \mathcal{D}\frac{\partial^2 x(t,\xi)}{\partial \xi^2} - \alpha(x(t,\xi))\left[\beta(x(t,\xi)) - \mathcal{P}(t,\xi) f(x(t,\xi))\right. \\ & \left. - \mathcal{Q}(t,\xi) g(x(t-\Im(t),\xi))\right], \end{aligned} \tag{8}$$

where the functions $\mathcal{P}(t,\xi)$ and $\mathcal{Q}(t,\xi)$ are expressed as convex combinations given by

$$\mathcal{P}(t,\xi)=\sum_{k=1}^{2^{2n^2}}\Omega_k(t)\mathcal{P}_k,\qquad \mathcal{Q}(t,\xi)=\sum_{k=1}^{2^{2n^2}}\Omega_k(t)\mathcal{Q}_k,$$

with $\Omega_k(t)$ being known weighting functions. In order to derive the main theoretical results, the following definitions, lemmas, and assumptions are introduced.

Due to the state-dependent switching property of the memristive synaptic weights, the system dynamics exhibit piecewise behavior. For analytical convenience, the switching system can be represented in an equivalent convex combination form, where the coefficients $\Omega_k(t)$ satisfy $\Omega_k(t)\geq 0$ and $\sum_{k=1}^{m}\Omega_k(t)=1$. These coefficients are introduced to characterize the convex hull of the possible subsystem dynamics and are used purely for analysis purposes.

Definition 1 ([1]). *The FOMRDCGNNs (1) are said to be asymptotically stable if the following condition holds:*

$$\lim_{t\to\infty}\|x(t,\xi)\|^2=0.$$

Definition 2 ([29]). *If FOMRDCGNNs (1) are asymptotically stable for all admissible uncertainties (i.e., $\Delta\mathcal{P}(t,\xi)$ and $\Delta\mathcal{Q}(t,\xi)$), then FOMRDCGNNs (1) are robust asymptotically stable.*

Lemma 1 ([11]). *As for a differentiable vector $x(t)\in\mathbb{R}^n$, we have*

$$_0^C\mathcal{D}_t^{\eta}\left[x^T(t)x(t)\right]\leq 2x^T(t)\,_0^C\mathcal{D}_t^{\eta}x(t),\forall\, 0<\eta<1,t\geq 0.$$

Lemma 2 ([37]). *Let $x\in W^{1,2}([l_1,l_2];\mathbb{R}^n)$ be a vector-valued function that satisfies $x(l_1)=0$ or $x(l_2)=0$. For any symmetric positive-definite matrix $\mathbf{M}\in\mathbb{R}^{n\times n}$,*

$$\int_{l_1}^{l_2}x^T(s)\,\mathbf{M}\,x(s)\,\mathrm{d}s\leq\frac{4(l_2-l_1)^2}{\pi^2}\int_{l_1}^{l_2}\left(\frac{\mathrm{d}x(s)}{\mathrm{d}s}\right)^T\mathbf{M}\left(\frac{\mathrm{d}x(s)}{\mathrm{d}s}\right)\mathrm{d}s.$$

Razumikhin-type condition: For the Lyapunov functional $V(t,x(t,\cdot))$, suppose that there exists a scalar constant $\mu>1$ such that for all $t\geq 0$, the following condition holds:

$$V(t+\theta,x(t+\theta,\cdot))\leq\mu V(t,x(t,\cdot)),\quad\forall\theta\in[-\tau,0].$$

Under this Razumikhin-type condition, the stability analysis can be carried out using the Lyapunov approach.

Lemma 3 ([24]). *The continuous function $\mathcal{V}(t,x(t,\cdot)):[0,+\infty)\times\mathbb{R}^n\to\mathbb{R}^+$ satisfies that, for $t>t_0$, continuous function ϕ, the following inequality holds:*

$$_0^CD_t^{\eta}\mathcal{V}(t,\phi(0,\cdot))\leq\epsilon\mathcal{V}(t,\phi(0,\cdot)),\ \epsilon\in\mathbb{R},\eta\in(0,1),$$

whenever $\mathcal{V}(t+\theta,\phi(\theta,\cdot))\leq\mathcal{V}(t,\phi(0,\cdot))$ for all $\theta\in[-\Im,0]$. Then

$$\mathcal{V}(t,x(t,\cdot))\leq\sup_{-\Im\leq\theta\leq 0}\mathcal{V}(0,\phi(\theta,\cdot))E_{\eta}\left(\epsilon(t-t_0)^{\eta}\right),t\geq t_0.$$

Lemma 4 ([26]). *For any value of η such that $0<\eta<1$, one has*

$$E_{\eta}(-\lambda\omega^{\eta})\leq\frac{\mathcal{N}}{1+\lambda\omega^{\eta}}\leq\frac{\mathcal{N}}{\lambda}\omega^{-\eta},t\geq 0,$$

where $\mathcal{N}$ is a positive constant and independent of ω.

Lemma 5 ([28]). *Let $0 < \wp < 1$. The Mittag–Leffler function $E_\wp(\omega)$ is non-negative. Moreover, for any $\omega_1 \geq \omega_2 \geq 0$, we have $E_\eta(-\omega_1) \leq E_\wp(-\omega_2)$ and $E_\wp(\omega_1) \geq E_\wp(\omega_2)$.*

Assumption 1. *There exist positive constants $\underline{\alpha}_i$ and $\overline{\alpha}_i$ such that, for all $x_i \in \mathbb{R}$ and $i = 1, 2, \ldots, n$, the amplification functions satisfy*

$$0 < \underline{\alpha}_i \leq \alpha_i(x_i) \leq \overline{\alpha}_i.$$

Assumption 2. *There exist positive constants ω_i $(i = 1, 2, \ldots, n)$ such that, for any $x, y \in \mathbb{R}$, the behavior functions satisfy*

$$(x - y)\big(\beta_i(x) - \beta_i(y)\big) \geq \omega_i (x - y)^{\mathrm{T}}(x - y).$$

Assumption 3. *There exist positive constants $\mathcal{C}_1$ and $\mathcal{C}_2$ such that, for all $x, y \in \mathbb{R}^n$, the activation functions satisfy the following Lipschitz-type conditions:*

(i)

$$[f(x) - f(y)]^{\mathrm{T}}[f(x) - f(y)] \leq \mathcal{C}_1 (x - y)^{\mathrm{T}}(x - y),$$

(ii)

$$[g(x) - g(y)]^{\mathrm{T}}[g(x) - g(y)] \leq \mathcal{C}_2 (x - y)^{\mathrm{T}}(x - y).$$

In addition, it is assumed that the initial values are given by $\beta(0) = f(0) = \rho(0) = 0$, which implies that system (1) has a trivial solution.

3. Main Results

This section deals with two cases: Section 3.1: There is no uncertainty in the FOMRDCGNNs. Section 3.2: There is uncertainty in the FOMRDCGNNs. Initially, an IBC is designed under boundary measurements. Then, some sufficient criteria are obtained (i.e., Theorems 1 and 2) such that FOMRDCGNNs (1) and uncertain FOMRDCGNNs (27) are asymptotically stable and robust asymptotically stable, respectively.

For simplicity, we use the following notations:

$$\underline{\mathcal{A}} = \mathrm{diag}\{\underline{\mathrm{ff}}_1, \underline{\mathrm{ff}}_2, \ldots, \underline{\mathrm{ff}}_\mathrm{n}\},\ \overline{\mathcal{A}} = \mathrm{diag}\{\overline{\mathrm{ff}}_1, \overline{\mathrm{ff}}_2, \ldots, \overline{\mathrm{ff}}_\mathrm{n}\},\ \mathcal{B} = \mathrm{diag}\{!_1, !_2, \ldots, !_\mathrm{n}\}.$$

3.1. Stabilization of FOMRDCGNNs

To realize the stabilization of FOMRDCGNNs (1), an IBC based on boundary measurements is designed as follows:

$$u(t) = \begin{cases} \mathcal{L}_1 \int_{l_1}^{l_2} x(t, \xi)\ \mathrm{d}\xi + \mathcal{L}_2 x(t, l_2), & t \in (m\gamma, m\gamma + \delta\gamma] \\ 0, & t \in (m\gamma + \delta\gamma, (m+1)\gamma). \end{cases} \tag{9}$$

Here, $\mathcal{L}_1 = \mathrm{diag}\{\mathcal{L}_{11}, \mathcal{L}_{12}, \ldots, \mathcal{L}_{1n}\}$ and $\mathcal{L}_2 = \mathrm{diag}\{\mathcal{L}_{21}, \mathcal{L}_{22}, \ldots, \mathcal{L}_{2n}\}$ denote the boundary control gain matrices, where $\mathcal{L}_{ij} \in \mathbb{R}^{n \times n}$. The index m is a non-negative integer taking values $m = 0, 1, 2, \ldots$. The parameters γ and δ represent the control period and the control duty ratio, respectively, satisfying $\gamma > 0$ and $0 < \delta < 1$. The objective is to appropriately select the control gains $\mathcal{L}_1$ and $\mathcal{L}_2$, together with the parameters γ and δ, such that the FOMRDCGNNs described in (1) are stabilized.

Remark 1. *Consider the Lyapunov functional*

$$V(t, x(t, \cdot)) = \int_{l_1}^{l_2} x^T(t, \xi) x(t, \xi)\, d\xi.$$

It is easy to verify that $V(t,x(t,\cdot)) \geq 0$ for all admissible states $x(t,\cdot)$ and $V(t,x(t,\cdot)) = 0$ if and only if $x(t,\xi) = 0$ for all $\xi \in [l_1,l_2]$. Moreover, $V(t,x(t,\cdot))$ is continuous and radially unbounded with respect to the L^2-norm of the state. Therefore, $V(t,x(t,\cdot))$ satisfies the positive definiteness condition and can be considered a valid Lyapunov functional for the stability analysis of the considered reaction–diffusion system.

Theorem 1. *Under Assumptions 1–3 and IBC (9), if there exist positive constants γ, δ, and matrices $\mathcal{L}_1, \mathcal{L}_2 \in \mathbb{R}^{n\times n}$ that satisfy the conditions*

$$(C_1) \quad \Xi = \begin{pmatrix} \Xi_{11} & \Xi_{12} \\ * & \Xi_{22} \end{pmatrix} \leq 0 \tag{10}$$

$$(C_2) \quad \delta\gamma > \Im \tag{11}$$

$$(C_3) \quad E_\eta(-\lambda_3(\delta\gamma - \Im)^\eta)E_\eta(\lambda_4(\gamma-\delta\gamma)^\eta) < 1 \tag{12}$$

where $\Xi_{11} = \Phi + \varepsilon_2 I_n + \mathrm{sym}(\mathcal{D}\mathcal{L}_1) + \left(\frac{1}{l_2-l_1}\right)\mathrm{sym}(\mathcal{D}\mathcal{L}_2), \Phi = -2\underline{\mathcal{A}}\mathcal{B} + \overline{\mathcal{A}}\mathcal{P}_k\mathcal{P}_k^T\overline{\mathcal{A}} + \overline{\mathcal{A}}\mathcal{Q}_k\mathcal{Q}_k^T\overline{\mathcal{A}} + \varepsilon_1 I_n$, $\Xi_{12} = -\mathcal{L}_1^T\mathcal{D} - \left(\frac{1}{l_2-l_1}\right)\mathrm{sym}(\mathcal{D}\mathcal{L}_2)$, $\Xi_{22} = \left(\frac{1}{l_2-l_1}\right)\mathrm{sym}(\mathcal{D}\mathcal{L}_2) - \frac{\pi^2}{2(l_2-l_1)}\mathcal{D} + \varepsilon_2 I_n$, $\lambda_4 = \lambda_2 + \varepsilon_2$, λ_2 and $-\lambda_3$ are the maximum eigenvalues of matrices Φ and Ξ, then the FOMRDCGNNs (1) are asymptotically stable.

Proof. Take $\mathcal{V}(t,x(t,\cdot)) = \int_{l_1}^{l_2} x^T x \, \mathrm{d}\xi$. Hereafter, for simplicity, the variable (t,ξ) is omitted and denoted as $x_\Im = x(t-\Im(t),\xi)$.
Case I: When $t \in (m\gamma, m\gamma+\delta\gamma)$, then Lemma 1 gives

$$\begin{aligned} {}^{C}_{m\gamma}\mathcal{D}_t^\eta \mathcal{V}(t,x(t,\cdot)) &= \int_{l_1}^{l_2} {}^{C}_{m\gamma}\mathcal{D}_t^\eta \left(x^T x\right)\mathrm{d}\xi \leq 2\int_{l_1}^{l_2} x^T {}^{C}_{m\gamma}\mathcal{D}_t^\eta x \, \mathrm{d}\xi \\ &= 2\int_{l_1}^{l_2} \sum_{k=1}^{2^{2n^2}} \Omega_k(t)\, x^T \left\{ \mathcal{D}\frac{\partial^2 x}{\partial\xi^2} - \alpha(x)\left(\beta(x) - \mathcal{P}_k f(x) - \mathcal{Q}_k g(x_\Im)\right)\right\}\mathrm{d}\xi. \end{aligned} \tag{13}$$

Employing the integration-by-parts formula together with the boundary conditions of (1), we obtain

$$\int_{l_1}^{l_2} x^T\mathcal{D}\frac{\partial^2 x}{\partial\xi^2}\mathrm{d}\xi = -\int_{l_1}^{l_2}\frac{\partial x^T}{\partial\xi}\mathcal{D}\frac{\partial x}{\partial\xi}\,\mathrm{d}\xi + x^T\mathcal{D}\frac{\partial x}{\partial\xi}\Big|_{\xi=l_1}^{\xi=l_2} = -\int_{l_1}^{l_2}\frac{\partial x^T}{\partial\xi}\mathcal{D}\frac{\partial x}{\partial\xi}\,\mathrm{d}\xi + x^T(t,l_2)\mathcal{D}\,u(t).$$

To apply Lemma 2, define the following transformation

$$\tilde{x}(t,\xi) = x(t,\xi) - x(t,l_2), \quad \xi \in [l_1,l_2].$$

It is easy to verify that $\tilde{x}(t,l_2) = 0$. Therefore, the boundary condition required in Lemma 2 is satisfied. By taking $\overline{x} = x - x(t,l_2)$, it follows that $\overline{x}(t,l_2) = 0$ and $\dfrac{\partial x}{\partial\xi} = \dfrac{\partial\overline{x}}{\partial\xi}$. Then, we have

$$\begin{aligned} \int_{l_1}^{l_2} x^T\mathcal{D}\frac{\partial^2 x}{\partial\xi^2}\,\mathrm{d}\xi &= \int_{l_1}^{l_2} x^T(t,l_2)\mathcal{D}\mathcal{L}_1 x\,\mathrm{d}\xi + x^T(t,l_2)\mathcal{D}\mathcal{L}_2 x(t,l_2) - \int_{l_1}^{l_2}\frac{\partial\overline{x}^T}{\partial\xi}\mathcal{D}\frac{\partial\overline{x}}{\partial\xi}\,\mathrm{d}\xi \\ &\leq \int_{l_1}^{l_2}\left[x^T(t,l_2)\mathcal{D}\mathcal{L}_1 x + \left(\frac{1}{l_2-l_1}\right)x^T(t,l_2)\mathcal{D}\mathcal{L}_2 x(t,l_2)\right. \\ &\quad \left. -\frac{\pi^2}{4(l_2-l_1)^2}\overline{x}^T\mathcal{D}\,\overline{x}\right]\mathrm{d}\xi. \end{aligned} \tag{14}$$

According to Assumptions 1 and 2, we obtain

$$\begin{aligned}-2x^T\alpha(x)\beta(x) =& -2\sum_{i=1}^{n} x_i\alpha_i(x_i)\beta_i(x_i)\\ =& -2\sum_{i=1}^{n}\alpha_i(x_i)[x_i\beta_i(x_i)]\\ \leq& -2\sum_{i=1}^{n}\underline{\alpha}_i\omega_i x_i^2\\ \leq& -2x^T\underline{\mathcal{A}}\mathcal{B}x. \end{aligned} \tag{15}$$

By Assumption 3, it follows that

$$\begin{aligned}2x^T\alpha(x)\mathcal{P}_k f(x) =& x^T\alpha(x)\mathcal{P}_k f(x) + f^T(x)\mathcal{P}_k^T\alpha^T(x)x\\ \leq& x^T\alpha(x)\mathcal{P}_k\mathcal{P}_k^T\alpha^T(x)x + f^T(x)f(x)\\ \leq& x^T\left[\,\overline{\mathcal{A}}\mathcal{P}_k\mathcal{P}_k^T\overline{\mathcal{A}} + \varepsilon_1 I_n\right]x \end{aligned} \tag{16}$$

and similarly

$$2x^T\alpha(x)\mathcal{Q}_k g(x_\Im) \leq x^T\overline{\mathcal{A}}\mathcal{Q}_k\mathcal{Q}_k^T\overline{\mathcal{A}}x + \varepsilon_2 x_\Im^T x_\Im. \tag{17}$$

Substituting the inequalities (14)–(17) into (13), one has

$$\begin{aligned}{}_{m\gamma}^{C}\mathcal{D}_t^{\eta}\mathcal{V}(t,x(t,\cdot)) \leq& \int_{l_1}^{l_2}\sum_{k=1}^{2^{2n^2}}\Omega_k(t)\Big[x^{\mathrm{T}}\left[-2\underline{\mathcal{A}}\mathcal{B} + \overline{\mathcal{A}}\mathcal{P}_k\mathcal{P}_k^T\overline{\mathcal{A}} + \overline{\mathcal{A}}\mathcal{Q}_k\mathcal{Q}_k^T\overline{\mathcal{A}} + \varepsilon_1 I_n\right]x\\ &+ 2x^T(t,l_2)\mathcal{D}\mathcal{L}_1 x + \left(\frac{2}{l_2-l_1}\right)x^T(t,l_2)\mathcal{D}\mathcal{L}_2 x(t,l_2)\\ &- \frac{\pi^2}{2(l_2-l_1)^2}\overline{x}^T\mathcal{D}\overline{x}\Big]\mathrm{d}\xi + \varepsilon_2\int_{l_1}^{l_2} x_\Im^T x_\Im\ \mathrm{d}\xi\\ \leq& \int_{l_1}^{l_2}\sum_{k=1}^{2^{2n^2}}\Omega_k(t)\Big[x^T\left[-2\underline{\mathcal{A}}\mathcal{B} + \overline{\mathcal{A}}\mathcal{P}\mathcal{P}^T\overline{\mathcal{A}} + \overline{\mathcal{A}}\mathcal{Q}\mathcal{Q}^T\overline{\mathcal{A}} + \varepsilon_1 I_n\right]x\\ &+ 2(x-\overline{x})^T\mathcal{D}\mathcal{L}_1 x + \left(\frac{2}{l_2-l_1}\right)(x-\overline{x})^T\mathcal{D}\mathcal{L}_2(x-\overline{x})\\ &- \frac{\pi^2}{2(l_2-l_1)}\overline{x}^T\mathcal{D}\overline{x}\Big]\mathrm{d}\xi + \varepsilon_2\int_{l_1}^{l_2} x_{\mathrm{r}}^T x_\Im\ \mathrm{d}\xi\\ \leq& \int_{l_1}^{l_2}\sum_{k=1}^{2^{2n^2}}\Omega_k(t)\begin{pmatrix}x\\ \overline{x}\end{pmatrix}^T\overline{\Xi}\begin{pmatrix}x\\ \overline{x}\end{pmatrix}\ \mathrm{d}\xi + \varepsilon_2\int_{l_1}^{l_2} x_\Im^{\mathrm{T}} x_\Im\ \mathrm{d}\xi \end{aligned}$$

where

$$\overline{\Xi} = \begin{pmatrix}\overline{\Xi}_{11} & -\mathcal{L}_1^T\mathcal{D} - \left(\frac{1}{l_2-l_1}\right)\mathrm{sym}(\mathcal{D}\mathcal{L}_2)\\ * & \left(\frac{1}{l_2-l_1}\right)\mathrm{sym}(\mathcal{D}\mathcal{L}_2) - \frac{\pi^2}{2(l_2-l_1)}\mathcal{D}\end{pmatrix}$$

where

$$\overline{\Xi}_{11} = -2\underline{\mathcal{A}}\mathcal{B} + \overline{\mathcal{A}}\mathcal{P}_k\mathcal{P}_k^{\mathrm{T}}\overline{\mathcal{A}} + \overline{\mathcal{A}}\mathcal{Q}_k\mathcal{Q}_k^{\mathrm{T}}\overline{\mathcal{A}} + \varepsilon_1 I_n + \mathrm{sym}(\mathcal{D}\mathcal{L}_1) + \frac{1}{l_2-l_1}\mathrm{sym}(\mathcal{D}\mathcal{L}_2).$$

Let $-\lambda_1$ and $-\lambda_3$ denote the maximum eigenvalues of the matrices $\overline{\Xi}$ and Ξ, respectively. From $\Xi \leq 0$ and $\overline{\Xi} = \Xi - \varepsilon_2 I < 0$, it follows that $-\lambda_3 \leq 0$ and

$$-\lambda_1 = -\lambda_3 - \varepsilon_2 < 0.$$

Consequently, the following inequality holds:

$$
\begin{aligned}
{}^{C}_{m\gamma}\mathcal{D}^{\eta}_{t}\mathcal{V}(t,x(t,\cdot)) &\leq -\lambda_1 \int_{l_1}^{l_2} \left(x^T x + \overline{x}^T \overline{x}\right) \mathrm{d}\xi + \varepsilon_2 \int_{l_1}^{l_2} x_{\Im}^T x_{\Im}\, \mathrm{d}\xi \\
&\leq -\lambda_1 \int_{l_1}^{l_2} x^T x\, \mathrm{d}\xi + \varepsilon_2 \sup_{-\Im\leq s\leq 0} \int_{l_1}^{l_2} x^T(t+s,\xi)x(t+s,\xi)\mathrm{d}\xi.
\end{aligned}
$$

The above inequality implies that

$$
\mathcal{V}(t+s,\xi(m\gamma+s,\cdot)) \leq \mathcal{V}(t,x(m\gamma,\cdot)),
$$

for all $t > m\gamma$ and $s \in [-\Im, 0]$.

$$
\begin{aligned}
{}^{C}_{m\gamma}\mathcal{D}^{\eta}_{t}\mathcal{V}(t,x(m\gamma,\cdot)) &\leq -\lambda_1 \int_{l_1}^{l_2} x^T(m\gamma,x)x(m\gamma,\xi)\mathrm{d}\xi \\
&\quad + \varepsilon_2 \sup_{-\Im\leq s\leq 0} \int_{l_1}^{l_2} x^T(m\gamma+s,\xi)x(m\gamma+s,\xi)\mathrm{d}\xi \\
&= -\lambda_1 \mathcal{V}(t,x(m\gamma,\cdot)) + \varepsilon_2 \sup_{-\Im\leq s\leq 0} \mathcal{V}(t+s,\xi(m\gamma+s,\cdot)) \\
&\leq -(\lambda_1-\varepsilon_2)\mathcal{V}(t,x(m\gamma,\cdot)) \\
&= -\lambda_3 \mathcal{V}(t,x(m\gamma,\cdot)).
\end{aligned}
$$

By applying Lemma 3, it can be concluded that, whenever $t \in (m\gamma,\, m\gamma+\delta\gamma]$,

$$
\mathcal{V}(t,x(t,\cdot)) \leq \sup_{-\Im\leq s\leq 0} \mathcal{V}(m\gamma,x(m\gamma+s,\cdot))E_{\eta}(-\lambda_3(t-m\gamma)^{\eta}) \tag{18}
$$

Case II: When $t \in (m\gamma+\delta\gamma, \gamma(m+1)]$, Lemma 1 gives

$$
\begin{aligned}
{}^{C}_{m\gamma+\delta\gamma}\mathcal{D}^{\eta}_{t}\mathcal{V}(t,x(t,\cdot)) &= \int_{l_1}^{l_2} {}^{C}_{m\gamma+\delta\gamma}\mathcal{D}^{\eta}_{t}\mathcal{V}\left(x^T x\right)\mathrm{d}\xi \leq 2\int_{l_1}^{l_2} x^T {}^{C}_{m\gamma+\delta\gamma}\mathcal{D}^{\eta}_{t}\mathcal{V}x\, \mathrm{d}\xi \\
&= 2\int_{l_1}^{l_2} \sum_{k=1}^{2^{2n^2}} \Omega_k(t)x^T\left[\mathcal{D}\frac{\partial^2 x}{\partial\xi^2} + \mathcal{P}_k f(x) + \mathcal{Q}_k g(x_{\Im})\right]\mathrm{d}\xi \\
&\leq \int_{l_1}^{l_2} \sum_{k=1}^{2^{2n^2}} \Omega_k(t)\left[x^T\Phi x + \varepsilon_2 x_{\Im}^T x_{\Im}\right]\mathrm{d}\xi \\
&\leq \lambda_2 \int_{l_1}^{l_2} x^T x\, \mathrm{d}\xi + \varepsilon_2 \sup_{-\Im\leq s\leq 0} \int_{l_1}^{l_2} x^T(t+s,\xi)x(t+s,\xi)\mathrm{d}\xi
\end{aligned}
$$

where λ_2 denotes the maximum eigenvalue of the matrix Φ.

From the above, we can write $\mathcal{V}(t+s,x(m\gamma+\delta\gamma+\, s,\cdot)) \leq \mathcal{V}(t,x(m\gamma+\delta\gamma,\cdot))$ for $t > m\gamma+\delta\gamma, s \in [-\Im, 0]$

$$
\begin{aligned}
{}^{C}_{m\gamma+\delta\gamma}\mathcal{D}^{\eta}_{t}\mathcal{V}(t,x(m\gamma+\delta\gamma,\cdot)) &\leq \lambda_2 \int_{l_1}^{l_2} x^T(m\gamma+\delta\gamma,\xi)x(m\gamma+\delta\gamma,\xi)\, \mathrm{d}\xi \\
&\quad + \varepsilon_2 \sup_{-\Im\leq s\leq 0} \int_{l_1}^{l_2} x^T(m\gamma+\delta\gamma+s,\xi)x(m\gamma+\delta\gamma+s,\xi)\, \mathrm{d}\xi \\
&= \lambda_2 \mathcal{V}(t,x(m\gamma+\delta\gamma,\cdot)) + \varepsilon_2 \sup_{-\Im\leq s\leq 0} \mathcal{V}(t+s,x(m\gamma+\delta\gamma+s,\cdot)) \\
&\leq (\lambda_2+\varepsilon_2)\mathcal{V}(t,x(m\gamma+\delta\gamma,\cdot)) \\
&= \lambda_4 \mathcal{V}(t,x(m\gamma+\delta\gamma,\cdot))
\end{aligned}
$$

Applying Lemma 3, we obtain that, for all $t \in (m\gamma+\delta\gamma,\, (m+1)\gamma]$,

$$\mathcal{V}(t, x(t,\cdot)) \leq \sup_{-\Im \leq s \leq 0} \mathcal{V}(m\gamma + \delta\gamma, x(m\gamma + \delta\gamma + s, \cdot)) E_\eta(\lambda_4 (t - m\gamma - \gamma\delta)^\eta). \tag{19}$$

Using (18) and (19) together with mathematical induction, we prove that the following inequalities hold for all $t \in (m\gamma,\, m\gamma + \delta\gamma]$, where $m = 0, 1, 2, \ldots$.

$$\begin{aligned}\mathcal{V}(t, x(t,\cdot)) \leq & \sup_{-\Im \leq \theta \leq 0} \mathcal{V}(0, x(\theta,\cdot)) \left[E_\eta(-\lambda_3(\delta\gamma - \Im)^\eta)\right]^m \\ & \times \left[E_\eta(\lambda_4(\gamma - \delta\gamma)^\eta)\right]^m E_\eta(-\lambda_3 (t - m\gamma)^\eta)\end{aligned} \tag{20}$$

and for $t \in (m\gamma + \delta\gamma, \gamma(m+1)], m = 0, 1, 2, \ldots$

$$\begin{aligned}\mathcal{V}(t, x(t,\cdot)) \leq & \sup_{-\Im \leq \theta \leq 0} \mathcal{V}(0, x(\theta,\cdot)) \left[E_\eta(-\lambda_3(\delta\gamma - \Im)^\eta)\right]^{m+1} \\ & \times \left[E_\eta(\lambda_4(\gamma - \gamma\delta)^\eta)\right]^m E_\eta(\lambda_4 (t - m\gamma - \delta\gamma)^\eta)\end{aligned} \tag{21}$$

First, we verify that the statement holds for $m = 0$. By applying (18) and (19), together with Lemma 5 and condition C2 in (11), it follows that for $t \in (0,\, \delta\gamma]$,

$$\mathcal{V}(t, x(t,\cdot)) \leq \sup_{-\Im \leq \theta \leq 0} \mathcal{V}(0, x(\theta,\cdot)) E_\eta(-\lambda_3 t^\eta)$$

and for $t \in (\delta\gamma, \gamma]$

$$\begin{aligned}\mathcal{V}(t, x(t,\cdot)) &\leq \sup_{-\Im \leq s \leq 0} \mathcal{V}(\gamma\delta, x(\delta\gamma + s, \cdot)) E_\eta(\lambda_4 (t - \delta\gamma)^\eta) \\ &\leq \sup_{-\Im \leq s \leq 0} \mathcal{V}(0, x(s,\cdot)) E_\eta(-\lambda_3(\gamma\delta + s)^\eta) E_\eta(\lambda_4 (t - \delta\gamma)^\eta) \\ &\leq \sup_{-\Im \leq s \leq 0} \mathcal{V}(0, x(s,\cdot)) E_\eta(-\lambda_3(\gamma\delta - \Im)^\eta) E_\eta(\lambda_4 (t - \delta\gamma)^\eta).\end{aligned}$$

The above corresponds to (20) and (21) when $m = 0$. Now, suppose that (20) and (21) are satisfied for $m = n - 1$, that is, for $t \in ((n-1)\gamma, (n-1)\gamma + \delta\gamma]$.

$$\begin{aligned}\mathcal{V}(t, x(t,\cdot)) \leq & \sup_{-\Im \leq \theta \leq 0} \mathcal{V}(0, x(\theta,\cdot)) \left[E_\eta(-\lambda_3(\delta\gamma - \Im)^\eta)\right]^{n-1} \\ & \times \left[E_\eta(\lambda_4(\gamma - \delta\gamma)^\eta)\right]^{n-1} E_\eta(-\lambda_3 (t - (n-1)\gamma)^\eta),\end{aligned} \tag{22}$$

for the second interval $t \in ((n-1)\gamma + \delta\gamma, n\gamma]$

$$\begin{aligned}\mathcal{V}(t, x(t,\cdot)) \leq & \sup_{-\Im \leq \theta \leq 0} \mathcal{V}(0, x(\theta,\cdot)) \left[E_\eta(-\lambda_3(\delta\gamma - \Im)^\eta)\right]^{n} \\ & \times \left[E_\eta(\lambda_4(\gamma - \delta\gamma)^\eta)\right]^{n-1} E_\eta(\lambda_4 (t - (n-1)\gamma - \delta\gamma)^\eta).\end{aligned} \tag{23}$$

From (18), (19), (22) and (23) with by Lemma 5, we get $t \in (n\gamma, n\gamma + \delta\gamma]$

$$\begin{aligned}\mathcal{V}(t, x(t,\cdot)) &\leq \sup_{-\Im \leq s \leq 0} \mathcal{V}(n\gamma, x(n\gamma + s, \cdot)) E_\eta(-\lambda_3 (t - n\gamma)^\eta) \\ &\leq \sup_{-\Im \leq s \leq 0} \mathcal{V}(0, x(\theta,\cdot)) \left[E_\eta(-\lambda_3(\delta\gamma - \Im)^\eta)\right]^{n} \\ &\quad \times \left[E_\eta(\lambda_4(\omega - \delta\gamma)^\eta)\right]^{n-1} E_\eta(\lambda_4 (n\gamma + s \\ &\quad -(n-1)\omega - \delta\gamma)^\eta) E_\eta(-\lambda_3 (t - n\gamma)^\eta) \\ &\leq \sup_{-\Im \leq s \leq 0} \mathcal{V}(0, x(\theta,\cdot)) \left[E_\eta(-\lambda_3(\delta\gamma - \Im)^\eta)\right]^{n} \\ &\quad \times \left[E_\eta(\lambda_4(\omega - \delta\gamma)^\eta)\right]^{n} E_\eta(-\lambda_3 (t - n\gamma)^\eta),\end{aligned}$$

and for $t \in (n\gamma + \delta\gamma, (n+1)\gamma]$

$$\begin{aligned}\mathcal{V}(t, x(t,\cdot)) &\leq \sup_{-\Im \leq s \leq 0} V(n\gamma + \delta\gamma, x(n\gamma + \delta\gamma + s, \cdot)) E_\eta(\lambda_4(t - n\gamma - \delta\gamma)^\eta) \\ &\leq \sup_{-\Im \leq s \leq 0} \mathcal{V}(0, x(\theta,\cdot)) \left[E_\eta(-\lambda_3(\delta\gamma - \Im)^\eta)\right]^n \left[E_\eta(\lambda_4(\omega - \delta\gamma)^\eta)\right]^n \\ &\quad \times E_\eta(-\lambda_3(n\gamma + \gamma\delta + s - n\gamma)^\eta) E_\eta(\lambda_4(t - n\gamma - \delta\gamma)^\eta) \\ &\leq \sup_{-\Im \leq s \leq 0} \mathcal{V}(0, x(\theta,\cdot)) \left[E_\eta(-\lambda_3(\delta\gamma - \Im)^\eta)\right]^{n+1} \\ &\quad \times \left[E_\eta(\lambda_4(\omega - \delta\gamma)^\eta)\right]^n E_\eta(\lambda_4(t - n\gamma - \delta\gamma)^\eta).\end{aligned}$$

This implies that (20) and (21) are valid for $m = n$. Hence, by mathematical induction, (20) and (21) hold for all $m = 0, 1, 2, \ldots$.

Furthermore, according to condition C_3 given in (12), for $t \in [m\gamma, m\gamma + \delta\gamma)$, equivalently, $(t/\gamma) - \delta < m \leq t/\gamma$. By Lemma 5, one has

$$E_\eta(-\lambda_3(t - m\gamma)^\eta) \leq E_\eta(-\lambda_3(m\gamma - m\gamma)^\eta) = 1.$$

Therefore, it follows that

$$\begin{aligned}\mathcal{V}(t, x(t,\cdot)) &\leq \sup_{-\Im \leq s \leq 0} \mathcal{V}(0, x(\theta,\cdot)) \left[E_\eta(-\lambda_3(\delta\gamma - \Im)^\eta) E_\eta(\lambda_4(\gamma - \delta\gamma)^\eta)\right]^m \\ &\leq \sup_{-\Im \leq s \leq 0} \mathcal{V}(0, x(\theta,\cdot)) \left[E_\eta(-\lambda_3(\delta\gamma - \Im)^\eta) E_\eta(\lambda_4(\gamma - \delta\gamma)^\eta)\right]^{\frac{L}{\gamma} - \delta}\end{aligned}$$

also, $t \in (m\gamma + \delta\gamma, (m+1)\gamma]$, it gives $(t/\gamma) < m + 1 \leq (t/\gamma) + 1 - \delta$, $E_\eta(\lambda_4(t - m\gamma - \delta\gamma)^\eta) \leq E_\eta(\lambda_4(\gamma - \delta\gamma)^\eta)$

$$\begin{aligned}\mathcal{V}(t, x(t,\cdot)) &\leq \sup_{-\Im \leq s \leq 0} \mathcal{V}(0, x(\theta,\cdot)) \left[E_\eta(-\lambda_3(\delta\gamma - \Im)^\eta) E_\eta(\lambda_4(\gamma - \delta\gamma)^\eta)\right]^{m+1} \\ &\leq \sup_{-\Im \leq s \leq 0} \mathcal{V}(0, x(\theta,\cdot)) \left[E_\eta(-\lambda_3(\delta\gamma - \Im)^\eta) E_\eta(\lambda_4(\gamma - \delta\gamma)^\eta)\right]^{\frac{t}{\gamma}} \\ &\leq \sup_{-\Im \leq s \leq 0} \mathcal{V}(0, x(\theta,\cdot)) \left[E_\eta(-\lambda_3(\delta\gamma - \Im)^\eta) E_\eta(\lambda_4(\gamma - \delta\gamma)^\eta)\right]^{\frac{t}{\gamma} - \delta}.\end{aligned}$$

From the above,

$$\mathcal{V}(t, x(t,\cdot)) \leq \sup_{-\Im \leq s \leq 0} \mathcal{V}(0, x(\theta,\cdot)) \left[E_\eta(-\lambda_3(\delta\gamma - \Im)^\eta) E_\eta(\lambda_4(\gamma - \delta\gamma)^\eta)\right]^{\frac{t}{\gamma} - \delta},\ t \geq 0$$

which means that

$$\|x(t,\cdot)\|^2 \leq \sup_{-\Im \leq s \leq 0} \|\varphi(s,\cdot)\|^2 \left[E_\eta(-\lambda_3(\delta\gamma - \Im)^\eta) E_\eta(\lambda_4(\gamma - \delta\gamma)^\eta)\right]^{\frac{l}{\gamma} - \delta} \to 0 \text{ as } t \to \infty$$

from condition *C*3. According to Definition 1, the FOMRDCGNNs (1) are asymptotically stable under IBC (9). □

Remark 2. *By setting $\delta = 1$ in the controller (9), the IBC is transformed into the following continuous-time boundary control law:*

$$u(t) = \mathcal{L}_1 \int_{l_1}^{l_2} x(t, \xi)\, \mathrm{d}\xi + \mathcal{L}_2 x(t, l_2). \tag{24}$$

As a consequence, a corollary concerning the stabilization of the FOMRDCGNNs (1) under boundary control can be directly derived from Theorem 1.

Corollary 1. *Under Assumptions 1–3 and BC (24), if there exist matrices $\mathcal{L}_1, \mathcal{L}_2 \in \mathbb{R}^{n\times n}$ such that condition (25) holds, then the FOMRDCGNNs (1) are asymptotically stable.*

Proof. Take $\mathcal{V}(t, x(t,\cdot)) = \int_{l_1}^{l_2} x^T x \, \mathrm{d}\xi$. Then, Lemma 1 gives

$$\begin{aligned}
{}_0^C\mathcal{D}_t^\eta \mathcal{V}(t, x(t,\cdot)) &= \int_{l_1}^{l_2} {}_0^C\mathcal{D}_t^\eta \left(x^T x\right) \mathrm{d}\xi \le 2\int_{l_1}^{l_2} x^T {}_0^C\mathcal{D}_t^\eta x \, \mathrm{d}\xi \\
&= 2\int_{l_1}^{l_2} x^T \left\{ \mathcal{D}\frac{\partial^2 x}{\partial \xi^2} - \alpha(x)\left(\beta(x) - \mathcal{P}f(x) - \mathcal{Q}g(x_\Im)\right)\right\} \mathrm{d}\xi. \qquad (25)
\end{aligned}$$

By employing arguments similar to those used in the preceding proof, one obtains

$$\begin{aligned}
{}_0^C\mathcal{D}_t^\eta \mathcal{V}(t, x(t,\cdot)) &\le \int_{l_1}^{l_2} \Bigg[x^{\mathrm{T}}\big[-2\underline{\mathcal{A}}\mathcal{B} + \overline{\mathcal{A}}\mathcal{P}\mathcal{P}^T\overline{\mathcal{A}} + \overline{\mathcal{A}}\mathcal{Q}\mathcal{Q}^T\overline{\mathcal{A}} + \varepsilon_1 I_n\big] x + 2x^T(t,l_2)\mathcal{D}\mathcal{L}_1 \, x \\
&\quad + \left(\frac{2}{l_2 - l_1}\right) x^T(t,l_2)\mathcal{D}\mathcal{L}_2 x(t,l_2) - \frac{\pi^2}{2(l_2-l_1)^2}\overline{x}^T\mathcal{D}\overline{x}\Bigg] \mathrm{d}\xi + \varepsilon_2 \int_{l_1}^{l_2} x_\Im^T x_\Im \, \mathrm{d}\xi \\
&\le \int_{l_1}^{l_2} \Bigg[x^T\big[-2\underline{\mathcal{A}}\mathcal{B} + \overline{\mathcal{A}}\mathcal{P}\mathcal{P}^T\overline{\mathcal{A}} + \overline{\mathcal{A}}\mathcal{Q}\mathcal{Q}^T\overline{\mathcal{A}} + \varepsilon_1 I_n\big] x + 2(x-\overline{x})^T\mathcal{D}\mathcal{L}_1 \, x \\
&\quad + \left(\frac{2}{l_2 - l_1}\right) (x-\overline{x})^T\mathcal{D}\mathcal{L}_2 (x-\overline{x}) - \frac{\pi^2}{2(l_2-l_1)}\overline{x}^T\mathcal{D}\overline{x}\Bigg] \mathrm{d}\xi + \varepsilon_2 \int_{l_1}^{l_2} x_{\mathrm{r}}^T x_\Im \, \mathrm{d}\xi \\
&\le \int_{l_1}^{l_2} \begin{pmatrix} x \\ \overline{x} \end{pmatrix}^T \overline{\Xi} \begin{pmatrix} x \\ \overline{x} \end{pmatrix} \mathrm{d}\xi + \varepsilon_2 \int_{l_1}^{l_2} x_\Im^{\mathrm{T}} x_\Im \, \mathrm{d}\xi
\end{aligned}$$

where

$$\overline{\Xi} = \begin{pmatrix} \overline{\Xi}_{11} & -\mathcal{L}_1^T\mathcal{D} - \left(\frac{1}{l_2-l_1}\right)\mathrm{sym}(\mathcal{D}\mathcal{L}_2) \\ * & \left(\frac{1}{l_2-l_1}\right)\mathrm{sym}(\mathcal{D}\mathcal{L}_2) - \frac{\pi^2}{2(l_2-l_1)}\mathcal{D} \end{pmatrix}$$

where $\overline{\Xi}_{11} = -2\underline{\mathcal{A}}\mathcal{B} + \overline{\mathcal{A}}\mathcal{P}\mathcal{P}^T\overline{\mathcal{A}} + \overline{\mathcal{A}}\mathcal{Q}\mathcal{Q}^T\overline{\mathcal{A}} + \varepsilon_1 I_n + \mathrm{sym}(\mathcal{D}\mathcal{L}_1) + \left(\frac{1}{l_2-l_1}\right)\mathrm{sym}(\mathcal{D}\mathcal{L}_2)$. Let $-\overline{\lambda}$ and $-\lambda$ denote the maximum eigenvalues of the matrices $\overline{\Xi}$ and Ξ, respectively. Since $\Xi \le 0$, it follows that $-\lambda \le 0$. Moreover, noting that $\overline{\Xi} = \Xi - \varepsilon_2 I < 0$, we obtain $-\overline{\lambda} = -\lambda - \varepsilon_2 < 0$. Consequently, it follows that

$$\begin{aligned}
{}_0^C\mathcal{D}_t^\eta \mathcal{V}(t, x(t,\cdot)) &\le -\overline{\lambda}\int_{l_1}^{l_2} \left(x^T x + \overline{x}^T\overline{x}\right)\mathrm{d}\xi + \varepsilon_2 \int_{l_1}^{l_2} x_\Im^T x_\Im \, \mathrm{d}\xi \\
&\le -\overline{\lambda}\int_{l_1}^{l_2} x^T x \, \mathrm{d}\xi + \varepsilon_2 \int_{l_1}^{l_2} x_\Im^T x_\Im \, \mathrm{d}\xi. \qquad (26)
\end{aligned}$$

From the above, we have $\mathcal{V}(t+s, \xi(s,\cdot)) \le \mathcal{V}(t, x(0,\cdot))$ for $t \ge 0, s \in [-\Im, 0]$

$$\begin{aligned}
{}_0^C\mathcal{D}_t^\eta \mathcal{V}(t, x(0,\cdot)) &\le -\overline{\lambda}\int_{l_1}^{l_2} x^T(0,\xi)x(0,\xi)\mathrm{d}\xi + \varepsilon_2 \sup_{-\Im\le s\le 0}\int_{l_1}^{l_2} x^T(s,\xi)x(s,\xi) \, \mathrm{d}\xi \\
&= -\overline{\lambda}\mathcal{V}(t, x(0,\cdot)) + \varepsilon_2 \sup_{-\Im\le s\le 0} \mathcal{V}(t+s, \xi(s,\cdot)) \\
&\le -(\overline{\lambda} - \varepsilon_2)\mathcal{V}(t, x(0,\cdot)) \\
&= -\lambda\mathcal{V}(t, x(0,\cdot)).
\end{aligned}$$

By using Lemmas 3 and 4, we can get

$$\begin{aligned}\mathcal{V}(t,x(t,\cdot)) &= \sup_{-\Im\le s\le 0}\mathcal{V}(0,x(s,\cdot))E_\eta(-\lambda t^\eta)\\ &= \sup_{-\Im\le s\le 0}\mathcal{V}(0,\varphi(s,\cdot))E_\eta(-\lambda t^\eta)\\ &\le \sup_{-\Im\le s\le 0}\mathcal{V}(0,\varphi(s,\cdot))\frac{\mathcal{N}}{\lambda}t^{-\eta},\ \ t\ge 0\end{aligned}$$

which means that

$$\|x(t,\cdot))\|^2 \le \left[\sup_{-\Im\le s\le 0}\|\varphi(s,\cdot)\|^2\frac{\mathcal{N}}{\lambda}t^{-\eta}\right]\to 0 \text{ as } t\to\infty$$

where $\mathcal{N}$ is constant not depending on x. Therefore, the FOMRCGNNs (1) are asymptotically stable under BC (24). □

Remark 3. *The parameter δ represents the operation ratio of the intermittent boundary controller within each control period. Specifically, the controller is activated only during a fraction δ of the total period, while it remains inactive during the remaining interval. By choosing $\delta < 1$, the number of control activations is reduced, which decreases the frequency of controller operation.*

3.2. Robust Mittag–Leffler Stabilization of Uncertain FOMRDCGNNs via IBC

In real-world applications of NNs, the performance of the system tends to be affected by parameter fluctuations, measurement errors, and external disturbances. For example, in the electronic implementation process, electronic component tolerances can cause variations in some critical parameters such as the weights of interconnections between neurons, communication delays, and neuron activation or release rates. Such uncertainties can compromise the performance of the system and even result in instability. Therefore, making sure that the NN shows stable behavior when subjected to such uncertain conditions is an essential demand.

This section focuses on the robust stabilization of uncertain FOMRDCGNNs. It is shown that the proposed IBC strategy continues to guarantee asymptotic stability even in the presence of system uncertainties. To this end, we consider the following class of uncertain FOMRDCGNNs with time-varying delays:

$$\begin{aligned}{}_0^C\mathcal{D}_t^\eta x(t,\xi) = \mathcal{D}\frac{\partial^2 x(t,\xi)}{\partial\xi^2} - \alpha(x(t,\xi))\Big[\beta(x(t,\xi)) - \{\mathcal{P}(x(t,\xi)) + \Delta\mathcal{P}(t,\xi)\}f(x(t,\xi))\\ - \{\mathcal{Q}(x(t,\xi)) + \Delta\mathcal{Q}(t,\xi)\}(x(t,\xi))g(x(t-\Im(t),\xi))\Big],\end{aligned} \tag{27}$$

where $\Delta\mathcal{P}(t,\xi)$ and $\Delta\mathcal{Q}(t,\xi)$ denote admissible parametric uncertainties, which are assumed to take the following form:

$$\begin{bmatrix}\Delta\mathcal{P}(t,\xi) & \Delta\mathcal{Q}(t,\xi)\end{bmatrix} = \mathcal{H}\,\mathcal{F}(t,\xi)\begin{bmatrix}\mathcal{E}_1 & \mathcal{E}_2\end{bmatrix}.$$

Here, $\mathcal{F}(t,\xi)$ is an unknown time-varying matrix satisfying the norm-bounded condition $\mathcal{F}^T(t,\xi)\mathcal{F}(t,\xi)\le I$, while $\mathcal{H}$, $\mathcal{E}_1$, and $\mathcal{E}_2$ are known constant matrices.

Based on conditions (4)–(7), the uncertain FOMRDCGNNs (27) can be equivalently expressed as follows:

$$
\begin{aligned}
{}_0^C\mathcal{D}_t^\eta x(t,\xi) = &\sum_{k=1}^{2^{2n^2}} \Omega_k(t)\Big[\mathcal{D}\frac{\partial^2 x(t,\xi)}{\partial\xi^2} - \alpha(x(t,\xi))\big[\beta(x(t,\xi)) - \{\mathcal{P}_k + \Delta\mathcal{P}(t,\xi)\}f(x(t,\xi))\\
&- \{\mathcal{Q}_k + \Delta\mathcal{Q}(t,\xi)\}g(x(t-\Im(t),\xi))\big]\Big]\\
= &\mathcal{D}\frac{\partial^2 x(t,\xi)}{\partial\xi^2} - \alpha(x(t,\xi))\big[\beta(x(t,\xi)) - \{\mathcal{P}(t,\xi) + \Delta\mathcal{P}(t,\xi)\}f(x(t,\xi))\\
&- \{\mathcal{Q}(t,\xi) + \Delta\mathcal{Q}(t,\xi)\}g(x(t-\Im(t),\xi))\big]. \qquad (28)
\end{aligned}
$$

Then, one has the theorem on the robust stabilization of FOMRDCGNNs (27) via IBC from Theorem 1.

Theorem 2. *Under Assumptions 1–3 and IBC (9), if there exist positive constants γ, δ, and matrices $\mathcal{L}_1, \mathcal{L}_2 \in \mathbb{R}^{n\times n}$ that satisfy the conditions*

$$
(\overline{C_1}) \quad \Pi = \begin{pmatrix} \Pi_{11} & \Pi_{12} \\ * & \Pi_{22} \end{pmatrix} \le 0 \qquad (29)
$$

$$
(\overline{C_2}) \quad \delta\gamma > \Im \qquad (30)
$$

$$
(\overline{C_3}) \quad E_\eta\big(-\overline{\lambda}_3(\delta\gamma - \Im)^\eta\big)E_\eta\big(\overline{\lambda}_4(\gamma-\delta\gamma)^\eta\big) < 1 \qquad (31)
$$

where $\Pi_{11} = \Psi + \varepsilon_2 I_n + \mathrm{sym}(\mathcal{D}\mathcal{L}_1) + \left(\frac{1}{l_2-l_1}\right)\mathrm{sym}(\mathcal{D}\mathcal{L}_2), \Psi = -2\underline{\mathcal{A}}\mathcal{B} + \overline{\mathcal{A}}\mathcal{P}_k\mathcal{P}_k^T\overline{\mathcal{A}} + \overline{\mathcal{A}}\mathcal{Q}_k\mathcal{Q}_k^T\overline{\mathcal{A}} + \varepsilon_1 I_n$, $\Pi_{12} = -\mathcal{L}_1^T\mathcal{D} - \left(\frac{1}{l_2-l_1}\right)\mathrm{sym}(\mathcal{D}\mathcal{L}_2)$, $\Pi_{22} = \left(\frac{1}{l_2-l_1}\right)\mathrm{sym}(\mathcal{D}\mathcal{L}_2) - \frac{\pi^2}{2(l_2-l_1)}\mathcal{D} + \varepsilon_2 I_n$, $\overline{\lambda}_4 = \overline{\lambda}_2 + \varepsilon_2$, *$\overline{\lambda}_2$ is the eigenvalue of Ψ and $-\overline{\lambda}_3$ is the eigenvalue of Π, then the uncertain FOMRDCGNNs (27) are robust asymptotically stable.*

Proof. Take $\mathcal{V}(t,x(t,\cdot)) = \int_{l_1}^{l_2} x^T x\,\mathrm{d}\xi$. When $t \in (m\gamma, m\gamma+\delta\gamma)$, then Lemma 1 gives

$$
\begin{aligned}
{}_{m\gamma}^C\mathcal{D}_t^\eta \mathcal{V}(t,x(t,\cdot)) = &\int_{l_1}^{l_2} {}_{m\gamma}^C\mathcal{D}_t^\eta\left(x^T x\right)\mathrm{d}\xi \le 2\int_{l_1}^{l_2} x^T {}_{m\gamma}^C\mathcal{D}_t^\eta x\,\mathrm{d}\xi\\
=&2\int_{l_1}^{l_2}\sum_{k=1}^{2^{2n^2}}\Omega_k(t)\,x^T\Big\{\mathcal{D}\frac{\partial^2 x}{\partial\xi^2} - \alpha(x)\big(\beta(x) - (\mathcal{P}_k + \Delta\mathcal{P})f(x)\\
&- (\mathcal{Q}_k + \Delta\mathcal{Q})g(x_\Im)\big)\Big\}\mathrm{d}\xi. \qquad (32)
\end{aligned}
$$

From the definition of uncertain parameters $\Delta\mathcal{P}$ and $\Delta\mathcal{Q}$, and using Assumption 3, we can get

$$
\begin{aligned}
2x^T\alpha(x)\Delta\mathcal{P}f(x) =&2x^T\alpha(x)\mathcal{H}\mathcal{F}\mathcal{E}_1 f(x)\\
\le&x^T\alpha(x)\mathcal{H}\mathcal{H}^T\alpha^T(x)x + f^T(x)\mathcal{E}_1^T\mathcal{F}^T\mathcal{F}\mathcal{E}_1 f(x)\\
\le&x^T\big[\,\overline{\mathcal{A}}\mathcal{H}\mathcal{H}^T\overline{\mathcal{A}} + \varepsilon_1\lambda_{\max}(\mathcal{E}_1^T\mathcal{E}_1)I_n\big]x \qquad (33)
\end{aligned}
$$

and similarly

$$
2x^T\alpha(x)\Delta\mathcal{Q}g(x_\Im) \le x^T\overline{\mathcal{A}}\mathcal{H}\mathcal{H}^T\overline{\mathcal{A}}x + \varepsilon_2\lambda_{\max}(\mathcal{E}_2^T\mathcal{E}_2)x_\Im^T x_\Im. \qquad (34)
$$

For the proof, see Appendix A. □

Consequently, a corollary on the robust stabilization of the FOMRDCGNNs (1) under boundary control can be established based on Theorem 2 and Corollary 1.

Corollary 2. *Under Assumptions 1–3 and BC (24), if there exist matrices $\mathcal{L}_1, \mathcal{L}_2 \in \mathbb{R}^{n\times n}$ such that condition (29) holds, then the uncertain FOMRDCGNNs (27) are robust asymptotically stable.*

Remark 4. *The stability properties of the proposed models are determined by control parameters such as the control period γ, the control-time ratio δ, and the delayed upper bound in time $\Im$. These parameters are important because they help to satisfy the sufficient stability conditions provided by Conditions (C_1) and (C_2) of Theorem 1, and for Conditions $(\bar{C}_1)$ and $(\bar{C}_2)$ of Theorem 2. In conjunction with Lemma 5, we observe that the stabilization process is more straightforward when the time delay $\Im$ is smaller and the $\delta\gamma$ is larger. This implies that stabilization is more likely to occur as the controller continues to operate. This conclusion is in accordance with the practical applications of engineering. In Section 4, a simulation will be conducted to verify the results of this analysis.*

Remark 5. *The conditions outlined in Theorems 1 and 2 are sufficient. This statement implies that the control law can stabilize the FOMRDCGNNs (1) if feasible solutions to the LMIs (10) and (29) exist. Specifically, control gain matrices $\mathcal{L}_1$ and $\mathcal{L}_2$ are available. Use the Matlab LMI toolbox (R2021a) to solve LMIs (10) and (29) and obtain control gain matrices $\mathcal{L}_1$ and $\mathcal{L}_2$.*

For a more detailed explanation of the implementation of the control approach proposed in this paper on the specific model, we have presented the algorithm in a flowchart (Figure 1).

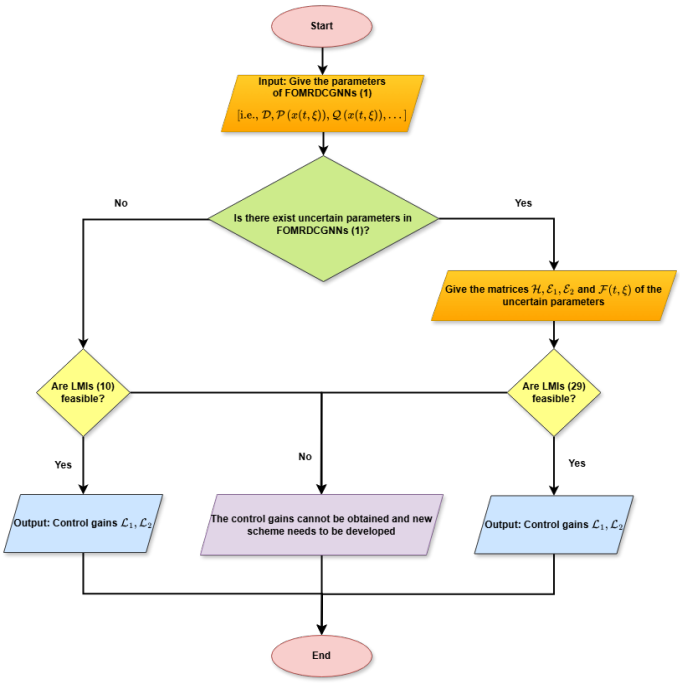


Figure 1. Flowchart algorithm of the developed control scheme.

4. Numerical Simulation

In this section, two numerical examples are provided to demonstrate the applicability and effectiveness of the theoretical results developed in this paper. Through simulation studies, these examples verify the feasibility of the proposed control strategy and highlight its capability in ensuring the desired stability performance of the considered systems.

Example 1. Consider a FOMRDCGNNs (1) with the parameters: $n = 3$, $\eta = 0.95$, $\xi \in (0,1)$, where the functions are specified as $\alpha(x(t,\xi)) = x(t,\xi)$, $\beta(x(t,\xi)) = 3x(t,\xi)$, $f(x(t,\xi)) = 0.8\tanh(x(t,\xi))$, $g(x(t-\Im(t),\xi)) = 0.4\tanh(x(t-\Im(t),\xi))$, $\Im(t) = 0.1 + 0.2\sin t$,

$$\mathcal{D} = \begin{pmatrix} 0.9 & 0 & 0 \\ 0 & 2 & 0 \\ 0 & 0 & 1 \end{pmatrix}, \ \mathcal{P}(x(t,\xi)) = \begin{pmatrix} -1 & p_{12}(x_1(t,\xi)) & p_{13}(x_1(t,\xi)) \\ p_{21}(x_2(t,\xi)) & -0.1 & p_{23}(x_2(t,\xi)) \\ p_{31}(x_3(t,\xi)) & p_{32}(x_3(t,\xi)) & 0.3 \end{pmatrix}, \text{ and}$$

$$\mathcal{Q}(x(t,\xi)) = \begin{pmatrix} 1 & q_{12}(x_1(t,\xi)) & q_{13}(x_1(t,\xi)) \\ q_{21}(x_2(t,\xi)) & -2.2 & q_{23}(x_3(t,\xi)) \\ q_{31}(x_3(t,\xi)) & q_{32}(x_3(t,\xi)) & -0.1 \end{pmatrix},$$

with

$$p_{12}(x_1(t,\xi)) = \begin{cases} 0.8, & \frac{\partial f_2(x_2(t,\xi))}{\partial t} - \frac{\partial x_1(t,\xi)}{\partial t} < 0, \\ 0.6, & \frac{\partial f_2(x_2(t,\xi))}{\partial t} - \frac{\partial x_1(t,\xi)}{\partial t} > 0, \end{cases}$$

$$p_{13}(x_1(t,\xi)) = \begin{cases} 0.4, & \frac{\partial f_3(x_3(t,\xi))}{\partial t} - \frac{\partial x_1(t,\xi)}{\partial t} < 0, \\ 0.2, & \frac{\partial f_3(x_3(t,\xi))}{\partial t} - \frac{\partial x_1(t,\xi)}{\partial t} > 0, \end{cases}$$

$$p_{21}(x_2(t,\xi)) = \begin{cases} -0.4, & \frac{\partial f_1(x_1(t,\xi))}{\partial t} - \frac{\partial x_2(t,\xi)}{\partial t} < 0, \\ -0.6, & \frac{\partial f_1(x_1(t,\xi))}{\partial t} - \frac{\partial x_2(t,\xi)}{\partial t} > 0, \end{cases}$$

$$p_{23}(x_2(t,\xi)) = \begin{cases} -0.1, & \frac{\partial f_3(x_3(t,\xi))}{\partial t} - \frac{\partial x_2(t,\xi)}{\partial t} < 0, \\ -0.3, & \frac{\partial f_3(x_3(t,\xi))}{\partial t} - \frac{\partial x_2(t,\xi)}{\partial t} > 0, \end{cases}$$

$$p_{31}(x_3(t,\xi)) = \begin{cases} -0.8, & \frac{\partial f_1(x_1(t,\xi))}{\partial t} - \frac{\partial x_3(t,\xi)}{\partial t} < 0, \\ 0.4, & \frac{\partial f_1(x_1(t,\xi))}{\partial t} - \frac{\partial x_3(t,\xi)}{\partial t} > 0, \end{cases}$$

$$p_{32}(x_3(t,\xi)) = \begin{cases} -0.4, & \frac{\partial f_2(x_2(t,\xi))}{\partial t} - \frac{\partial x_3(t,\xi)}{\partial t} < 0, \\ 0.8, & \frac{\partial f_2(x_2(t,\xi))}{\partial t} - \frac{\partial x_3(t,\xi)}{\partial t} > 0, \end{cases}$$

$$q_{12}(x_1(t,\xi)) = \begin{cases} -0.1, & \frac{\partial g_2(x_2(t-\Im(t),\xi))}{\partial t} - \frac{\partial x_1(t,\xi)}{\partial t} < 0, \\ -0.5, & \frac{\partial g_2(x_2(t-\Im(t),\xi))}{\partial t} - \frac{\partial x_1(t,\xi)}{\partial t} > 0, \end{cases}$$

$$q_{13}(x_1(t,\xi)) = \begin{cases} -0.1, & \frac{\partial g_3(x_3(t-\Im(t),\xi))}{\partial t} - \frac{\partial x_1(t,\xi)}{\partial t} < 0, \\ 0.3, & \frac{\partial g_3(x_3(t-\Im(t),\xi))}{\partial t} - \frac{\partial x_1(t,\xi)}{\partial t} > 0, \end{cases}$$

$$q_{21}(x_2(t,\xi)) = \begin{cases} 0.4, & \frac{\partial g_1(x_1(t-\Im(t),\xi))}{\partial t} - \frac{\partial x_2(t,\xi)}{\partial t} < 0, \\ -2.3, & \frac{\partial g_1(x_1(t-\Im(t),\xi))}{\partial t} - \frac{\partial x_2(t,\xi)}{\partial t} > 0, \end{cases}$$

$$q_{23}(x_2(t,\xi)) = \begin{cases} 0.5, & \frac{\partial g_3(x_3(t-\Im(t),\xi))}{\partial t} - \frac{\partial x_2(t,\xi)}{\partial t} < 0, \\ 1, & \frac{\partial g_3(x_3(t-\Im(t),\xi))}{\partial t} - \frac{\partial x_2(t,\xi)}{\partial t} > 0, \end{cases}$$

$$q_{31}(x_3(t,\xi)) = \begin{cases} -1, & \frac{\partial g_1(x_1(t-\Im(t),\xi))}{\partial t} - \frac{\partial x_3(t,\xi)}{\partial t} < 0, \\ 1.4, & \frac{\partial g_1(x_1(t-\Im(t),\xi))}{\partial t} - \frac{\partial x_3(t,\xi)}{\partial t} > 0, \end{cases}$$

$$q_{32}(x_3(t,\xi)) = \begin{cases} -1.4, & \frac{\partial g_2(x_2(t-\Im(t),\xi))}{\partial t} - \frac{\partial x_3(t,\xi)}{\partial t} < 0, \\ -0.2, & \frac{\partial g_2(x_2(t-\Im(t),\xi))}{\partial t} - \frac{\partial x_3(t,\xi)}{\partial t} > 0, \end{cases}$$

and an initial condition, for $\theta \in [-0.3, 0]$

$$\begin{cases} x_1(\theta,\xi) = 0.05(2-\cos(2\pi\xi))(\sin(\pi\theta - 0.1)), \\ x_2(\theta,\xi) = 0.02(2-\cos(3\pi\xi))(\sin(1.1\pi\theta - 0.1)), \\ x_2(\theta,\xi) = 0.08(1.5-\cos(1.5\pi\xi))(\sin(0.8\pi\theta - 0.2)). \end{cases}$$

A direct calculation gives $\overline{\mathcal{A}} = \underline{\mathcal{A}} = \text{diag}\{1,1,1\}$, $\mathcal{B} = \text{diag}\{3,3,3\}$, $\varepsilon_1 = 0.64$, and $\varepsilon_2 = 0.16$. Using the MATLAB LMI Toolbox to solve the matrix inequality (10) presented in Theorem 1, the following control gain matrices are achieved:

$$\mathcal{L}_1 = \begin{pmatrix} -39.0305 & 0 & 0 \\ 0 & -39.0305 & 0 \\ 0 & 0 & -39.0305 \end{pmatrix}, \mathcal{L}_2 = \begin{pmatrix} -26.2065 & 0 & 0 \\ 0 & -26.2065 & 0 \\ 0 & 0 & -26.2065 \end{pmatrix}.$$

The control period and the control-time ratio are chosen as $\gamma = 1.2$ and $\delta = 0.45$, respectively. The feasibility of Theorem 1 confirms that the FOMRDCGNNs described by (1) achieve theoretical stabilization under the designed controller (9). The state responses $x_i(t,\xi)$, $(i = 1,2,3)$ and the state norm $\|x(t,\xi\|^2$ under the controller (9) are depicted in Figure 2, which ensures that the FOMRDCGNNs (1) achieve stabilization. Let $u(t) = 0$ be illustrated that the controller (9) is effective. Figure 3 illustrates the responses of the uncontrolled state and the corresponding state norm, demonstrating that the FOMRDCGNNs (1) are unable to achieve stabilization. Thus, the proposed controller is valid. The time response of the control input (9) is presented in Figure 4.

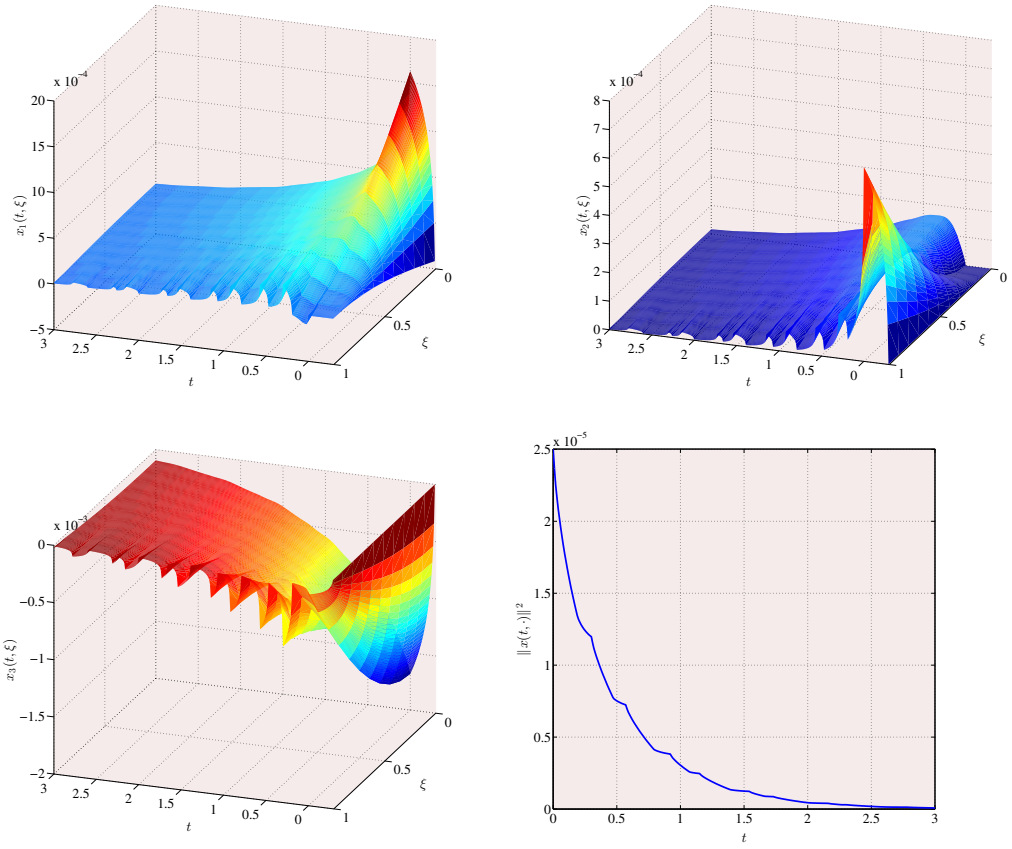


Figure 2. State responses $x(t,\xi)$ and state norm $\|x(t,\cdot)\|^2$ of FOMRDCGNNs (1) with IBC (9).

To understand the impact of fractional-order η, the system is configured for $\eta = 0.95$ and $\eta = 0.97$, keeping all other parameters fixed. As illustrated in Figure 5a, the speed of convergence improves with larger values of η. Next, to assess control-time length, δ is set to 0.6 with γ being 1.2. Figure 5b shows the evolution of the state norms over time with control-time ratios of $\delta = 0.3$ and $\delta = 0.5$. The state norm is observed to drop more rapidly when $\delta = 0.5$, as opposed to when $\delta = 0.3$. This shows that a longer control time contributes positively to the stabilization performance of FOMRDCGNNs (1). Therefore, the figure shows that the extension of the control time improves the stabilization

capabilities of FOMRDCGNNs (1) with respect to the expected performance. Finally, to analyze the impact of time delay, the delay function is taken as $\Im(t) = 0.8 + 0.4\sin(t)$ with $\Im = 1.2$, while the other parameters remain the same. In this case, the stability conditions in Theorem 2 are not satisfied. The variation in the state norm for the two time delay functions with $\Im(t) = 0.1 + 0.2\sin(t)$ and $\Im(t) = 0.8 + 0.4\sin(t)$ is illustrated in Figure 5c. The system with the smaller delay reaches stability quickly, whereas the system with the larger delay does so slowly and remains unstable. This confirms that shorter time delays enhance the stabilization performance of the FOMRDCGNN system.

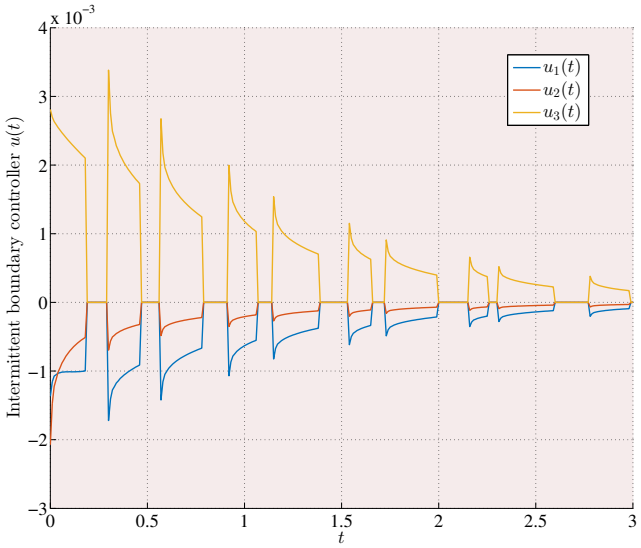


Figure 3. Time responses of IBC (9) with FOMRDCGNNs (1).

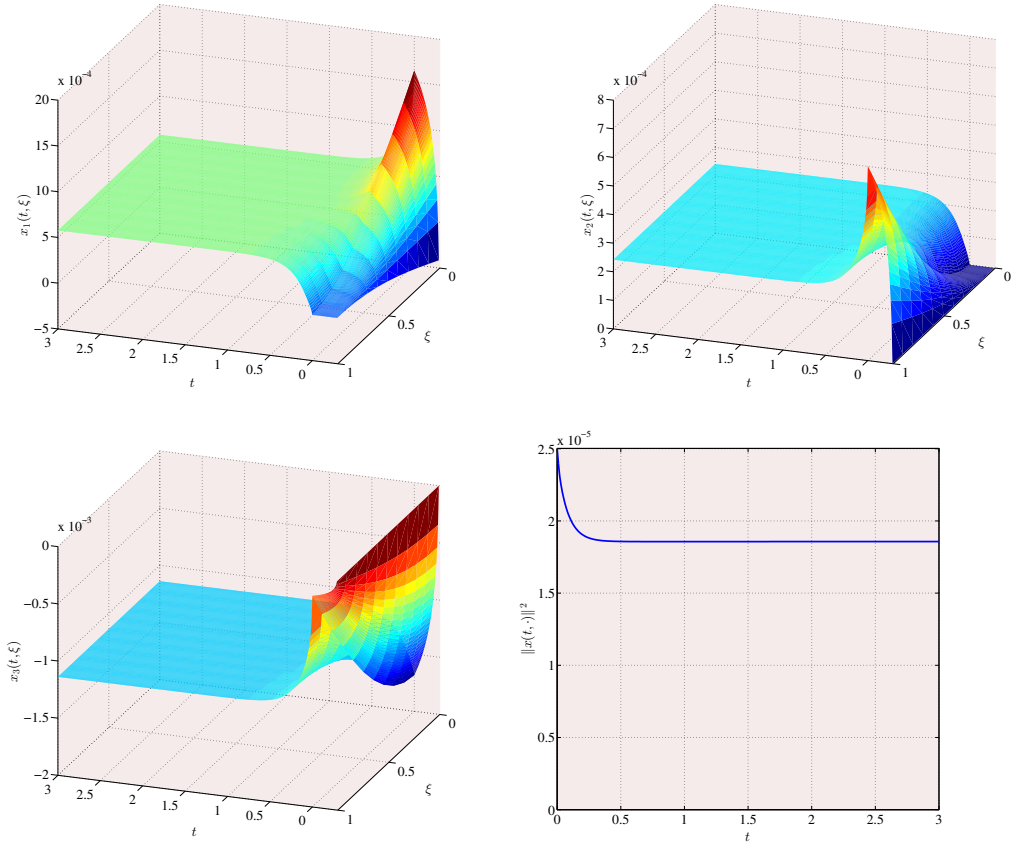


Figure 4. State responses $x(t,\xi)$ and state norm $\|x(t,\cdot)\|^2$ of FOMRDCGNNs (1) without control.

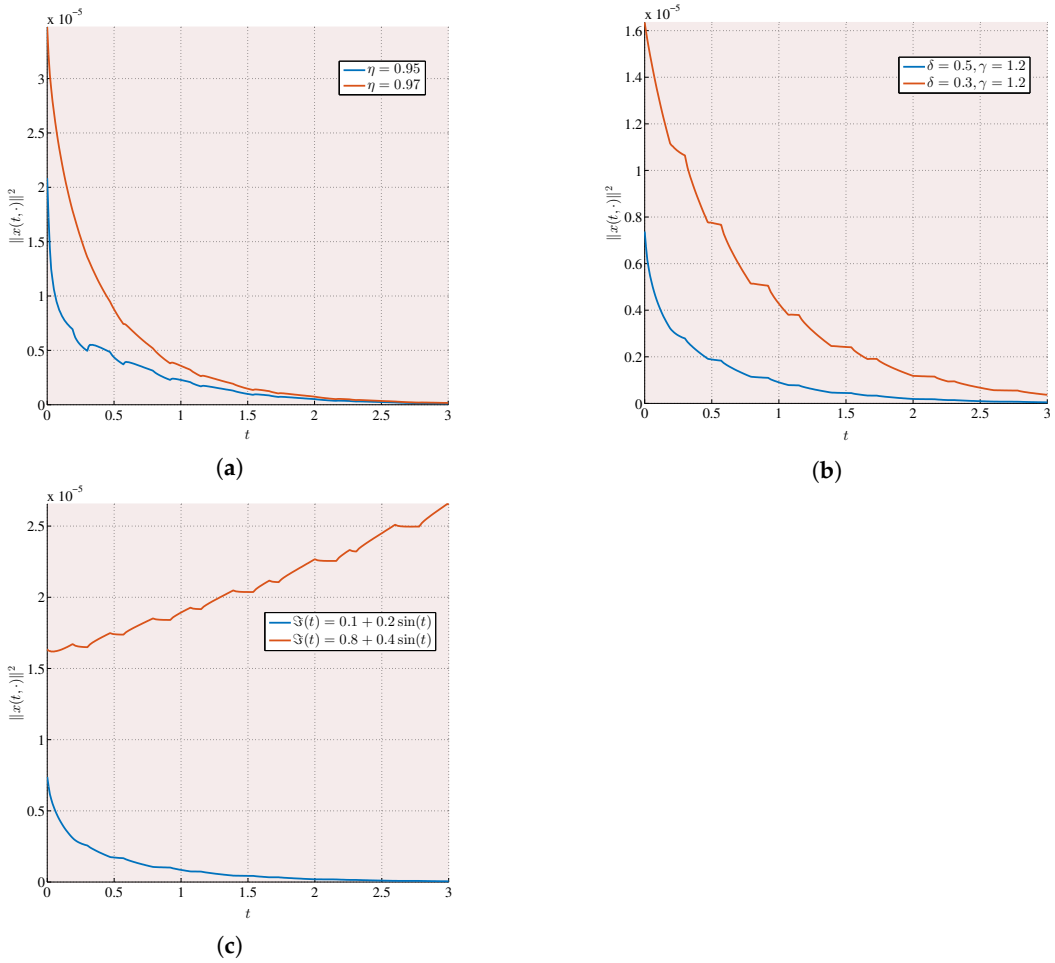


Figure 5. State norm $\|x(t,\cdot)\|^2$ of FOMRDCGNNs (1): (**a**) different parameter η, (**b**) different control-time length, and (**c**) different delays.

Remark 6. *The feasibility of the derived stability conditions is verified by solving the corresponding LMIs using the MATLAB LMI Toolbox. Once feasible solutions are obtained, numerical simulations are carried out in MATLAB to generate the state trajectories and graphical results presented in this section. These simulations illustrate the effectiveness of the proposed control scheme.*

Example 2. Consider uncertain FOMRDCGNNs (27) with the details of the uncertainties $\Delta\mathcal{P}(t,\xi)$ and $\Delta\mathcal{Q}(t,\xi)$ expressed as follows:

$$\mathcal{H} = \begin{pmatrix} 0.05 & 0 & 0 \\ 0 & 0.05 & 0 \\ 0 & 0 & 0.05 \end{pmatrix}, \ \mathcal{E}_1 = \mathcal{E}_2 = \begin{pmatrix} 0.4 & 0 & 0 \\ 0 & 0.2 & 0 \\ 0 & 0 & 0.2 \end{pmatrix},$$

$$\mathcal{F}(t,\xi) = \begin{pmatrix} \cos(t) & \sin(t) & 0 \\ -\sin(t) & \cos(t) & 0 \\ 0 & 0 & \xi \end{pmatrix},$$

and the remaining parameters are the same as in Example 1. Solving the LMI (29) in Theorem 2 gives the following control gain matrices:

$$\mathcal{L}_1 = \begin{pmatrix} -38.8763 & 0 & 0 \\ 0 & -38.8763 & 0 \\ 0 & 0 & -38.8763 \end{pmatrix}, \ \mathcal{L}_2 = \begin{pmatrix} -26.1007 & 0 & 0 \\ 0 & -26.1007 & 0 \\ 0 & 0 & -26.1007 \end{pmatrix}.$$

The control-time period $\gamma = 1$, and the control-time ratio $\delta = 0.56$. We see that Theorem 2 holds, which ensures that uncertain FOMRDCGNNs (27) are theoretically stabilized under the controller (9). Figure 6 shows the state responses $x_i(t,\xi)$, $(i = 1,2,3)$, and the state norm $\|x(t,\xi)\|^2$ under the controller (24), which ensures that the uncertain FOMRDCGNN (27) is robustly stabilized. The effectiveness of the designed controller is confirmed by its time-response performance. Figure 7 illustrates the dynamic behavior of the controller in (9) with uncertain FOMRDCGNNs described in (27).

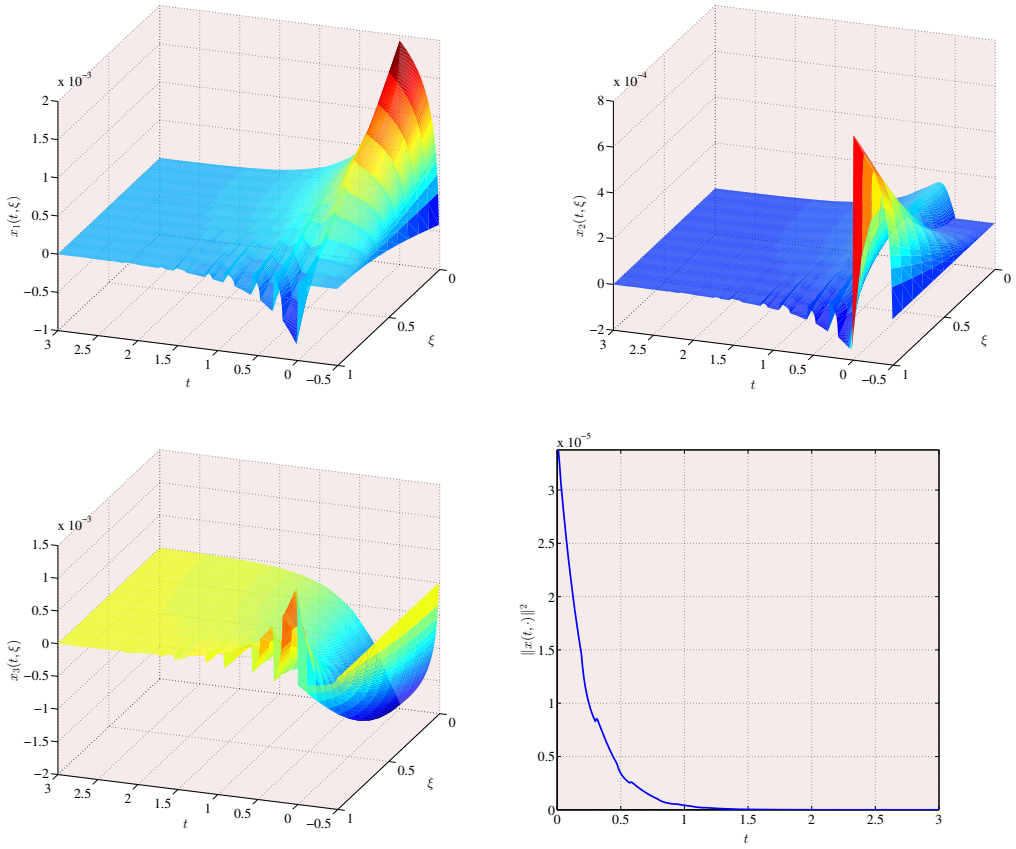


Figure 6. State responses $x(t,\xi)$ and state norm $\|x(t,\cdot)\|^2$ of uncertain FOMRDCGNNs (27) with IBC (9).

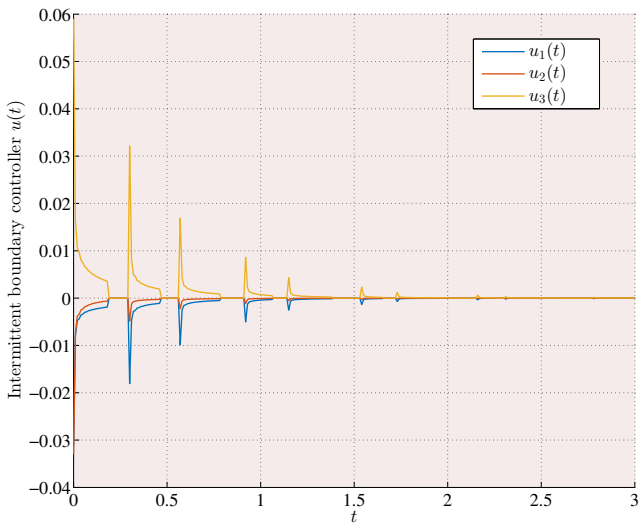


Figure 7. Time responses of IBC (9) with uncertain FOMRDCGNNs (27).

5. Conclusions

This paper investigated the robust stabilization problem of FOMRDCGNNs with time-varying delays under an intermittent boundary control (IBC) framework. The proposed IBC strategy effectively reduces control effort by requiring actuation only over limited time intervals and at the boundary of the spatial domain. By constructing appropriate Lyapunov functionals and integrating the IBC mechanism, sufficient conditions were derived to guarantee asymptotic stability for the nominal system (Theorem 1) and robust asymptotic stability in the presence of parametric uncertainties (Theorem 2). Numerical simulation results confirmed the theoretical analysis, and two illustrative examples further demonstrated the feasibility and effectiveness of the proposed control scheme. The developed results provide a practical and efficient approach for stabilizing fractional-order reaction–diffusion neural networks and may be extended to more complex network structures and control constraints in future studies.

Author Contributions: Conceptualization, M.M. and S.S.; methodology, M.M. and S.S.; software, M.M. and S.S.; validation, S.R. and M.R.; formal analysis, M.R.; investigation, S.S.; resources, S.R.; writing—original draft preparation, M.M. and S.S.; writing—review and editing, S.R. and M.R.; visualization, S.S.; supervision, S.R. and M.R. All authors have read and agreed to the published version of the manuscript.

Funding: The authors extend their appreciation to the Ongoing Research Funding Program (ORF-2026-683), King Saud University, Riyadh, Saudi Arabia.

Data Availability Statement: Since no new data were produced or analyzed in this research, data availability is not applicable.

Conflicts of Interest: The authors declare no conflicts of interest.

Nomenclature

Notation	Description
$\mathbb{R}$	The set of real numbers
$\mathbb{R}^+$	The positive real number space
$\mathbb{R}^n$	Euclidean space of dimensional n
$\mathbb{R}^{n\times n}$	Real-valued matrix of dimensions $n \times n$
I_n	Identity matrix of dimension n
$\mathrm{diag}\{\cdot\}$	Diagonal matrix
$A > 0 (< 0)$	Positive (negative) definite matrix A
A^T	Transpose of a matrix A
A^{-1}	Inverse of a matrix A
$\lambda_{\min}(\cdot)$	Minimum eigenvalue of matrix
$\lambda_{\max}(\cdot)$	Maximum eigenvalue of matrix
$*$	Symmetric term of matrix
$\mathrm{sym}(A)$	$A + A^{\mathrm{T}}$
$W^{1,2}([l_1, l_2]; \mathbb{R}^n)$	Sobolev space of absolutely continuous functions
$\|x(t,\xi)\|^2$	$\int_{l_1}^{l_2} x^T(t,\xi)x(t,\xi)d\xi$

Appendix A

From Theorem 1 substituting the inequalities (14)–(17), (33) and (34) into (32), one has

$$
\begin{aligned}
{}_{m\gamma}^{C}\mathcal{D}_t^{\eta}\mathcal{V}(t,x(t,\cdot)) \le & \int_{l_1}^{l_2} \sum_{k=1}^{2^{2n^2}} \Omega_k(t)\Big[x^{\mathrm{T}}\big[-2\underline{\mathcal{A}}\mathcal{B}+2\overline{\mathcal{A}}\mathcal{H}\mathcal{H}^T\overline{\mathcal{A}}+\overline{\mathcal{A}}\mathcal{P}_k\mathcal{P}_k^T\overline{\mathcal{A}}+\overline{\mathcal{A}}\mathcal{Q}_k\mathcal{Q}_k^T\overline{\mathcal{A}} \\
& +\varepsilon_1\lambda_{\max}(\mathcal{E}_1^T\mathcal{E}_1)I_n\big]x+2x^T(t,l_2)\mathcal{D}\mathcal{L}_1x+\left(\frac{2}{l_2-l_1}\right)x^T(t,l_2)\mathcal{D}\mathcal{L}_2x(t,l_2) \\
& -\frac{\pi^2}{2(l_2-l_1)^2}\overline{x}^T\mathcal{D}\overline{x}\Big]\mathrm{d}\xi+\varepsilon_2\lambda_{\max}(\mathcal{E}_2^T\mathcal{E}_2)\int_{l_1}^{l_2}x_{\Im}^Tx_{\Im}\,\mathrm{d}\xi \\
\le & \int_{l_1}^{l_2} \sum_{k=1}^{2^{2n^2}} \Omega_k(t)\Big[x^T\big[-2\underline{\mathcal{A}}\mathcal{B}+\overline{\mathcal{A}}\mathcal{P}\mathcal{P}^T\overline{\mathcal{A}}+\overline{\mathcal{A}}\mathcal{Q}\mathcal{Q}^T\overline{\mathcal{A}}+\varepsilon_1 I_n\big]x \\
& +2(x-\overline{x})^T\mathcal{D}\mathcal{L}_1x+\left(\frac{2}{l_2-l_1}\right)(x-\overline{x})^T\mathcal{D}\mathcal{L}_2(x-\overline{x}) \\
& -\frac{\pi^2}{2(l_2-l_1)}\overline{x}^T\mathcal{D}\overline{x}\Big]\mathrm{d}\xi+\varepsilon_2\lambda_{\max}(\mathcal{E}_2^T\mathcal{E}_2)\int_{l_1}^{l_2}x_{\mathrm{r}}^Tx_{\Im}\,\mathrm{d}\xi \\
\le & \int_{l_1}^{l_2} \sum_{k=1}^{2^{2n^2}} \Omega_k(t)\begin{pmatrix}x\\ \overline{x}\end{pmatrix}^T\overline{\Pi}\begin{pmatrix}x\\ \overline{x}\end{pmatrix}\,\mathrm{d}\xi+\varepsilon_2\lambda_{\max}(\mathcal{E}_2^T\mathcal{E}_2)\int_{l_1}^{l_2}x_{\Im}^Tx_{\Im}\,\mathrm{d}\xi
\end{aligned}
$$

where

$$
\overline{\Pi}=\begin{pmatrix}\overline{\Pi}_{11} & -\mathcal{L}_1^T\mathcal{D}-\left(\frac{1}{l_2-l_1}\right)\mathrm{sym}(\mathcal{D}\mathcal{L}_2)\\ * & \left(\frac{1}{l_2-l_1}\right)\mathrm{sym}(\mathcal{D}\mathcal{L}_2)-\frac{\pi^2}{2(l_2-l_1)}\mathcal{D}\end{pmatrix}
$$

with $\overline{\Pi}_{11}=-2\underline{\mathcal{A}}\mathcal{B}+2\overline{\mathcal{A}}\mathcal{H}\mathcal{H}^T\overline{\mathcal{A}}+\overline{\mathcal{A}}\mathcal{P}_k\mathcal{P}_k^T\overline{\mathcal{A}}+\overline{\mathcal{A}}\mathcal{Q}_k\mathcal{Q}_k^T\overline{\mathcal{A}}+\varepsilon_1\lambda_{\max}(\mathcal{E}_1^T\mathcal{E}_1)I_n+\mathrm{sym}(\mathcal{D}\mathcal{L}_1)+\left(\frac{1}{l_2-l_1}\right)\mathrm{sym}(\mathcal{D}\mathcal{L}_2)$. Let $-\lambda_1$ and $-\lambda_3$ denote the maximum eigenvalues of the matrices $\overline{\Pi}$ and Π, respectively. Then we have $-\overline{\lambda}_3\le 0$ and $-\overline{\lambda}_1=-\overline{\lambda}_3-\varepsilon_2<0$, since $\Pi\le 0$ and $\overline{\Pi}=\Pi-\varepsilon_2 I<0$, and it follows that

$$
\begin{aligned}
{}_{m\gamma}^{C}\mathcal{D}_t^{\eta}\mathcal{V}(t,x(t,\cdot)) &\le -\overline{\lambda_1}\int_{l_1}^{l_2}\left(x^Tx+\overline{x}^T\overline{x}\right)\mathrm{d}\xi+\varepsilon_2\int_{l_1}^{l_2}x_{\Im}^Tx_{\Im}\,\mathrm{d}\xi \\
&\le -\lambda_1\int_{l_1}^{l_2}x^Tx\,\mathrm{d}\xi+\varepsilon_2\sup_{-\Im\le s\le 0}\int_{l_1}^{l_2}x^T(t+s,\xi)x(t+s,\xi)\mathrm{d}\xi.
\end{aligned}
$$

From the above, we can get $\mathcal{V}(t+s,\xi(m\gamma+s,\cdot))\le\mathcal{V}(t,x(m\gamma,\cdot))$ for $t>m\gamma, s\in[-\Im,0]$

$$
\begin{aligned}
{}_{m\gamma}^{C}\mathcal{D}_t^{\eta}\mathcal{V}(t,x(m\gamma,\cdot)) &\le -\overline{\lambda}_1\int_{l_1}^{l_2}x^T(m\gamma,x)x(m\gamma,\xi)\mathrm{d}\xi \\
&\quad+\varepsilon_2\sup_{-\Im\le s\le 0}\int_{l_1}^{l_2}x^T(m\gamma+s,\xi)x(m\gamma+s,\xi)\mathrm{d}\xi \\
&=-\overline{\lambda}_1\mathcal{V}(t,x(m\gamma,\cdot))+\varepsilon_2\sup_{-\Im\le s\le 0}\mathcal{V}(t+s,\xi(m\gamma+s,\cdot)) \\
&\le-(\overline{\lambda}_1-\varepsilon_2)\mathcal{V}(t,x(m\gamma,\cdot)) \\
&=-\overline{\lambda}_3\mathcal{V}(t,x(m\gamma,\cdot)).
\end{aligned}
$$

For $t\in(m\gamma,m\gamma+\delta\gamma]$, we get

$$
\mathcal{V}(t,x(t,\cdot))\le\sup_{-\Im\le s\le 0}\mathcal{V}(m\gamma,x(m\gamma+s,\cdot))E_{\eta}\big(-\overline{\lambda}_3(t-m\gamma)^{\eta}\big). \tag{A1}
$$

Similarly, when $t\in(m\gamma+\delta\gamma,\gamma(m+1)]$, Lemma 1 gives

$$
\begin{aligned}
{}^{C}_{m\gamma+\delta\gamma}\mathcal{D}^{\eta}_{t}\mathcal{V}(t,x(t,\cdot)) &= \int_{l_1}^{l_2} {}^{C}_{m\gamma+\delta\gamma}\mathcal{D}^{\eta}_{t}\mathcal{V}\left(x^{T}x\right)\mathrm{d}\xi \le 2\int_{l_1}^{l_2} x^{T}\,{}^{C}_{m\gamma+\delta\gamma}\mathcal{D}^{\eta}_{t}\mathcal{V}x\,\mathrm{d}\xi \\
&= 2\int_{l_1}^{l_2}\sum_{k=1}^{2^{2n^2}}\Omega_k(t)x^{T}\left[\mathcal{D}\frac{\partial^2 x}{\partial\xi^2}+(\mathcal{P}_k+\Delta\mathcal{P})f(x)+(\mathcal{Q}_k+\Delta\mathcal{Q})g(x_{\Im})\right]\mathrm{d}\xi \\
&\le \int_{l_1}^{l_2}\sum_{k=1}^{2^{2n^2}}\Omega_k(t)\left[x^{T}\Psi x+\varepsilon_2 x_{\Im}^{T}x_{\Im}\right]\mathrm{d}\xi \\
&\le \overline{\lambda}_2\int_{l_1}^{l_2}x^{T}x\,\mathrm{d}\xi+\varepsilon_2\sup_{-\Im\le s\le 0}\int_{l_1}^{l_2}x^{T}(t+s,\xi)x(t+s,\xi)\mathrm{d}\xi
\end{aligned}
$$

where $\overline{\lambda}_2$ denotes the maximum eigenvalue of the matrix Ψ.

From the above analysis, it follows that $\mathcal{V}(t+s,x(m\gamma+\delta\gamma+s,\cdot)) \le \mathcal{V}(t,x(m\gamma+\delta\gamma,\cdot))$ for $t > m\gamma+\delta\gamma, s\in[-\Im,0]$

$$
\begin{aligned}
{}^{C}_{m\gamma+\delta\gamma}\mathcal{D}^{\eta}_{t}\mathcal{V}(t,x(m\gamma+\delta\gamma,\cdot)) &\le \overline{\lambda}_2\int_{l_1}^{l_2}x^{T}(m\gamma+\delta\gamma,\xi)x(m\gamma+\delta\gamma,\xi)\,\mathrm{d}\xi \\
&\quad+\varepsilon_2\sup_{-\Im\le s\le 0}\int_{l_1}^{l_2}x^{T}(m\gamma+\delta\gamma+s,\xi)x(m\gamma+\delta\gamma+s,\xi)\,\mathrm{d}\xi \\
&= \overline{\lambda}_2\mathcal{V}(t,x(m\gamma+\delta\gamma,\cdot))+\varepsilon_2\sup_{-\Im\le s\le 0}\mathcal{V}(t+s,x(m\gamma+\delta\gamma+s,\cdot)) \\
&\le (\overline{\lambda}_2+\varepsilon_2)\mathcal{V}(t,x(m\gamma+\delta\gamma,\cdot)) \\
&= \overline{\lambda}_4\mathcal{V}(t,x(m\gamma+\delta\gamma,\cdot))
\end{aligned}
$$

For $t\in(m\gamma+\delta\gamma,\gamma(m+1)]$, we get

$$
\mathcal{V}(t,x(t,\cdot)) \le \sup_{-\Im\le s\le 0}\mathcal{V}(m\gamma+\delta\gamma,x(m\gamma+\delta\gamma+s,\cdot))E_{\eta}\left(\overline{\lambda}_4(t-m\gamma-\gamma\delta)^{\eta}\right). \tag{A2}
$$

Following the analytical procedure established in Theorem 1, one can derive

$$
\|x(t,\cdot)\|^2 \le \sup_{-\Im\le s\le 0}\|\varphi(s,\cdot)\|^2\left[E_{\eta}(-\lambda_3(\delta\gamma-\Im)^{\eta})E_{\eta}(\lambda_4(\gamma-\delta\gamma)^{\eta})\right]^{\frac{I}{\gamma}-\delta}\to 0 \text{ as } t\to\infty.
$$

According to Definition 2, the uncertain FOMRDCGNNs (27) are robust asymptotically stable under IBC (9).

References

1. Gholami, Y. Globally asymptotic stability analysis for memristor-based competitive systems of reaction–diffusion delayed neural networks. *Math. Methods Appl. Sci.* **2023**, *46*, 17036–17064. [CrossRef]
2. Kim, Y.H.; Lewis, F.L.; Dawson, D.M. Intelligent optimal control of robotic manipulators using neural networks. *Automatica* **2000**, *36*, 1355–1364. [CrossRef]
3. Lakshmanan, S.; Prakash, M.; Lim, C.P.; Rakkiyappan, R.; Balasubramaniam, P.; Nahavandi, S. Synchronization of an inertial neural network with time-varying delays and its application to secure communication. *IEEE Trans. Neural Netw. Learn. Syst.* **2016**, *29*, 195–207. [CrossRef]
4. Hagan, M.T.; Demuth, H.B.; Jesús, O.D. An introduction to the use of neural networks in control systems. *Int. J. Robust Nonlinear Control IFAC-Affil. J.* **2002**, *12*, 959–985. [CrossRef]
5. Thakkar, A.; Chaudhari, K. A comprehensive survey on deep neural networks for stock market: The need, challenges, and future directions. *Expert Syst. Appl.* **2021**, *177*, 114800. [CrossRef]
6. Yegnanarayana, B. Artificial neural networks for pattern recognition. *Sadhana* **1994**, *19*, 189–238. [CrossRef]
7. Joya, G.; Atencia, M.; Sandoval, F. Hopfield neural networks for optimization: Study of the different dynamics. *Neurocomputing* **2002**, *43*, 219–237. [CrossRef]

8. Liu, Z.; Liao, L. Existence and global exponential stability of periodic solution of cellular neural networks with time-varying delays. *J. Math. Anal. Appl.* **2004**, *290*, 247–262. [CrossRef]
9. Zhang, H.; Wang, Z.; Liu, D. A comprehensive review of stability analysis of continuous-time recurrent neural networks. *IEEE Trans. Neural Netw. Learn. Syst.* **2014**, *25*, 1229–1262. [CrossRef]
10. Cohen, M.A.; Grossberg, S. Absolute stability of global pattern formation and parallel memory storage by competitive neural networks. *IEEE Trans. Syst. Man Cybern.* **1983**, *SMC-13*, 815–826. [CrossRef]
11. Zhou, Z. Stability and synchronization of delayed fractional-order reaction-diffusion Cohen-Grossberg neural networks under perturbation and parameter mismatch. *Asian J. Control* **2025**. [CrossRef]
12. Kao, Y.; Cao, Y.; Chen, X. Global Mittag–Leffler synchronization of coupled delayed fractional reaction-diffusion Cohen-Grossberg neural networks via sliding mode control. *Chaos Interdiscip. J. Nonlinear Sci.* **2022**, *32*, 113123. [CrossRef]
13. Aravind, R.V.; Balasubramaniam, P. Stability criteria for memristor-based delayed fractional-order Cohen–Grossberg neural networks with uncertainties. *J. Comput. Appl. Math.* **2023**, *420*, 114764. [CrossRef]
14. Fan, Y.; Wang, Z. A review for dynamic analysis and control of memristive neural networks. *Nonlinear Dyn.* **2024**, *113*, 5939–5952. [CrossRef]
15. Nie, X.; Zheng, W.X.; Cao, J. Multistability of memristive Cohen-Grossberg neural networks with non-monotonic piecewise linear activation functions and time-varying delays. *Neural Netw.* **2015**, *71*, 27–36. [CrossRef]
16. Hui, M.; Luo, N.; Wu, Q.; Yao, R.; Bai, L. New results of finite-time synchronization via piecewise control for memristive Cohen-Grossberg neural networks with time-varying delays. *IEEE Access* **2019**, *7*, 79173–79185. [CrossRef]
17. Zheng, M.; Li, L.; Peng, H.; Xiao, J.; Yang, Y.; Zhao, H. Finite-time stability and synchronization for memristor-based fractional-order Cohen-Grossberg neural network. *Eur. Phys. J. B* **2016**, *89*, 204. [CrossRef]
18. Hui, M.; Wei, C.; Zhang, J.; Iu, H.H.C.; Luo, N.; Yao, R.; Bai, L. Finite-time synchronization of memristor-based fractional order Cohen-Grossberg neural networks. *IEEE Access* **2020**, *8*, 73698–73713. [CrossRef]
19. Du, F.; Lu, J.G. Novel methods of finite-time synchronization of fractional-order delayed memristor-based Cohen-Grossberg neural networks. *Nonlinear Dyn.* **2023**, *111*, 18985–19001. [CrossRef]
20. Kong, F.; Zhu, Q.; Karimi, H.R. Fixed-time periodic stabilization of discontinuous reaction–diffusion Cohen-Grossberg neural networks. *Neural Netw.* **2023**, *166*, 354–365. [CrossRef] [PubMed]
21. Dharani, S.; Rakkiyappan, R.; Park, J.H. Pinning sampled-data synchronization of coupled inertial neural networks with reaction-diffusion terms and time-varying delays. *Neurocomputing* **2017**, *227*, 101–107. [CrossRef]
22. Dong, T.; Xia, L. Spatial temporal dynamic of a coupled reaction-diffusion neural network with time delay. *Cogn. Comput.* **2019**, *11*, 212–226. [CrossRef]
23. Hu, D.; Tan, J.; Shi, K.; Ding, K. Switching synchronization of reaction-diffusion neural networks with time-varying delays. *Chaos Solitons Fractals* **2022**, *155*, 111766. [CrossRef]
24. Stamova, I.M.; Simeonov, S. Delayed reaction–diffusion cellular neural networks of fractional order: Mittag–Leffler stability and synchronization. *J. Comput. Nonlinear Dyn.* **2018**, *13*, 011015. [CrossRef]
25. Li, R.; Cao, J.; Li, N. Stabilization of reaction–diffusion fractional-order memristive neural networks. *Neural Netw.* **2023**, *165*, 290–297. [CrossRef]
26. Liu, X.Z.; Wu, K.N.; Ahn, C.K. Intermittent boundary control for synchronization of fractional delay neural networks with diffusion terms. *IEEE Trans. Syst. Man Cybern. Syst.* **2022**, *53*, 2900–2912. [CrossRef]
27. Ali, M.S.; Saravanan, S.; Palanisamy, L. Stochastic finite-time stability of reaction-diffusion Cohen–Grossberg neural networks with time-varying delays. *Chin. J. Phys.* **2019**, *57*, 314–328. [CrossRef]
28. Stamova, I.; Stamov, G. Mittag–Leffler synchronization of fractional neural networks with time-varying delays and reaction–diffusion terms using impulsive and linear controllers. *Neural Netw.* **2017**, *96*, 22–32. [CrossRef] [PubMed]
29. Li, R.; Cao, J. Stability analysis of reaction-diffusion uncertain memristive neural networks with time-varying delays and leakage term. *Appl. Math. Comput.* **2016**, *278*, 54–69. [CrossRef]
30. Cao, Y.; Kao, Y.; Wang, Z.; Yang, X.; Park, J.H.; Xie, W. Sliding mode control for uncertain fractional-order reaction–diffusion memristor neural networks with time delays. *Neural Netw.* **2024**, *178*, 106402. [CrossRef]
31. Wang, H.; Liu, S.; Wu, X.; Sun, J.; Qiao, W. Stability of Fractional Reaction-Diffusion Memristive Neural Networks Via Event-Based Hybrid Impulsive Controller. *Neural Process. Lett.* **2024**, *56*, 79. [CrossRef]
32. Wei, A.; Wang, K.; Wang, E.; Tong, T. Finite-time stabilization for semi-Markov reaction–diffusion memristive NNs: A boundary pinning control scheme. *Knowl.-Based Syst.* **2023**, *266*, 110409. [CrossRef]
33. Stamova, I.; Stamov, G. On the stability of sets for reaction–diffusion Cohen–Grossberg delayed neural networks. *Discret. Contin. Dyn. Syst.-Ser. S* **2021**, *14*, 1429–1446. [CrossRef]
34. Ren, F.; Jiang, M.; Xu, H.; Fang, X. New finite-time synchronization of memristive Cohen–Grossberg neural network with reaction–diffusion term based on time-varying delay. *Neural Comput. Appl.* **2021**, *33*, 4315–4328. [CrossRef]

35. Stamova, I.; Stamov, T.; Stamov, G. Lipschitz stability analysis of fractional-order impulsive delayed reaction-diffusion neural network models. *Chaos Solitons Fractals* **2022**, *162*, 112474. [CrossRef]
36. Gokulakrishnan, V.; Srinivasan, R. Event-Triggered controller on practically exponential input-to-state stabilization of stochastic reaction-diffusion Cohen-Grossberg neural networks and its application to image encryption. *Neural Process. Lett.* **2023**, *55*, 11147–11171. [CrossRef]
37. Liu, X.Z.; Wu, K.N.; Ding, X.; Zhang, W. Boundary stabilization of stochastic delayed Cohen-Grossberg neural networks with diffusion terms. *IEEE Trans. Neural Netw. Learn. Syst.* **2021**, *33*, 3227–3237. [CrossRef]
38. Abudireman, A.; Abdurahman, A.; Jiang, H. Fixed-time synchronization of spatiotemporal Cohen-Grossberg neural networks via aperiodic intermittent control. *Commun. Nonlinear Sci. Numer. Simul.* **2025**, *150*, 108991. [CrossRef]
39. Wang, Y.; Chen, W.H.; Niu, S.; Lu, X. Stabilization of delayed stochastic reaction-diffusion Cohen-Grossberg neural networks via variable gain intermittent boundary control. *Neural Netw.* **2025**, *193*, 108041. [CrossRef] [PubMed]
40. Liu, X.Z.; Wu, K.N.; Zhang, W. Intermittent boundary stabilization of stochastic reaction-diffusion Cohen-Grossberg neural networks. *Neural Netw.* **2020**, *131*, 1–13. [CrossRef] [PubMed]

Disclaimer/Publisher's Note: The statements, opinions and data contained in all publications are solely those of the individual author(s) and contributor(s) and not of MDPI and/or the editor(s). MDPI and/or the editor(s) disclaim responsibility for any injury to people or property resulting from any ideas, methods, instructions or products referred to in the content.